Calcium-permeable AMPA receptors mediate timing-dependent LTP elicited by 6 coincident action potentials at Schaffer collateral-CA1 synapses

Running title: Modulation of threshold t-LTP

Efrain A. Cepeda-Prado[1#], Babak Khodaie[1,3#], Gloria D. Quiceno[1], Swantje Beythien[1], Volkmar Leßmann[1,2,3,Δ,*], Elke Edelmann[1,2,3*]

[1]Institut für Physiologie, Otto-von-Guericke-Universität, Medizinische Fakultät, Leipziger Str. 44, 39120 Magdeburg, Germany

[2]Center for Behavioral Brain Sciences, Magdeburg, Germany

[3]OVGU International ESF-funded Graduate School ABINEP, Magdeburg, Germany

[#] shared first authorship, * Shared senior authorship

[Δ] correspondence: lessmann@med.ovgu.de

Keywords:

spike timing-dependent plasticity, STDP, hippocampus, dopamine, calcium, BDNF, t-LTP

Abstract

Activity-dependent synaptic plasticity in neuronal circuits represents a cellular model of memory formation. Such changes can be elicited by repeated high-frequency stimulation inducing long-term potentiation (LTP), or by low frequency stimulation induced long-term depression (LTD). Spike timing-dependent plasticity (STDP) can induce equally robust long-lasting timing-dependent LTP (t-LTP) in response to low frequency repeats of coincident action potential (AP) firing in presynaptic cells followed by postsynaptic neurons. Conversely, this stimulation can lead to t-LTD if the postsynaptic spike precedes the presynaptic action potential. STDP is best suited to investigate synaptic plasticity mechanisms at the single cell level. Commonly, STDP paradigms relying on 25-100 repeats of coincident pre- and postsynaptic firing are used to elicit t-LTP or t-LTD. However, the minimum number of repeats required for successful STDP induction, which could account for fast single trial learning *in vivo*, is barely explored. Here, we examined low repeat STDP at Schaffer collateral-CA1 synapses by pairing one presynaptic AP with either one postsynaptic AP (1:1 t-LTP) or a burst of 4 APs (1:4 t-LTP). We found 3-6 repeats to be sufficient to elicit t-LTP. Postsynaptic Ca^{2+} elevation for 1:1 t-LTP required NMDARs and VGCCs, while 1:4 t-LTP depended on metabotropic GluR and ryanodine receptor signaling. Surprisingly, both 6x t-LTP variants were strictly dependent on activation of postsynaptic Ca^{2+}-permeable AMPARs. Both t-LTP forms were regulated differentially by dopamine receptors, but occurred independent from BDNF/TrkB signaling. Our data show that synaptic changes induced by only 3-6 repeats of mild STDP stimulation occuring in ≤10 s can take place on time scales observed also during single trial learning.

Introduction

Long-term potentiation (LTP) and long-term depression (LTD) of synaptic transmission can be observed in response to repetitive activation of synapses and are believed to represent cellular models of learning and memory processes in the brain (see e.g., Bi and Poo, 1998; Bliss and Cooke, 2011; Malenka and Bear, 2004). While LTP leads to a stable enhancement of synaptic transmission between connected neurons, LTD yields a long-lasting decrease in synaptic responses. Depending on the time frame that is investigated, LTP as well as LTD can be divided into an early phase lasting roughly 1h and a late phase that starts 2-3h after induction of the synaptic change. While early LTP is mediated by posttranslational modifications, late LTP was found to depend on synthesis of new proteins (Lynch, 2004; but see Wang et al., 2016). LTP was initially discovered using long-lasting high frequency stimulation of glutamatergic synapses in the mammalian hippocampus (Bliss and Lomo, 1973), a brain region essential for encoding episodic memory (Tonegawa et al., 2018). While in these pioneering studies, LTP was recorded *in vivo* using extracellular field potential recordings (Bliss and Lomo, 1973), LTP is also observed in acutely isolated brain slices *ex vivo* and can be recorded in individual neurons using whole cell patch clamp recording techniques (reviewed e.g. in Herring and Nicoll, 2016; Lalanne et al., 2018; Pinar et al., 2017). Notably, LTP studies at the single cell level are essential to understand the biochemical and cellular mechanisms of LTP and LTD processes of a specific neuronal connection with defined postsynaptic target. To relate results from LTP measurements in acute slices *ex vivo* with learning processes it is important to use LTP induction protocols that resemble synaptic activation patterns also occurring during memory formation *in vivo* (compare Bittner et al., 2015; 2017; Otto et al., 1991), rather than paradigms involving tetanic synaptic stimulation or long-lasting artificial depolarization of postsynaptic neurons.

In this respect, spike timing-dependent plasticity (STDP) seems to represent an especially relevant protocol for induction of LTP (e.g., Bi and Poo, 2001; Caporale and Dan, 2008; Costa et al., 2017; Edelmann et al., 2017; Edelmann et al., 2014; Feldman, 2012; Markram et al., 2011). Here, bidirectional plasticity can be induced by repeated coincident activation of pre- and postsynaptic neurons, with forward pairing (i.e. presynaptic spike occurs several ms before the postsynaptic action potential; positive spike timing (+Δt)) yielding timing-dependent (t-) LTP, while backward pairing (postsynaptic spike occurs before presynaptic activation; -Δt) yields t-LTD. These protocols also fulfill the prerequisites for Hebbian synaptic plasticity (Caporale and Dan, 2008) that are widely accepted as fundamental requirements for synaptic plasticity. Compared to pairing protocols that induce LTP by combining a presynaptic tetanus with a postsynaptic depolarization (e.g., Meis et al., 2012), STDP relies on a small number of pre- and postsynaptic action potentials that are repeated at low frequency (< 5 Hz).

Like memory formation *in vivo*, t-LTP in acute *ex vivo* brain slices is strongly controlled by neuromodulatory inputs, which can regulate the efficacy of induction paradigms to elicit plasticity (Edelmann and Lessmann, 2011, 2013; reviewed in Edelmann and Lessmann, 2018; Liu et al., 2017; Pawlak and Kerr, 2008; e.g., Seol et al., 2007). Such kind of neuromodulation can also bridge the temporal gap between synaptic plasticity and behavioral time scales for learning processes (Gerstner et al., 2018; Shindou et al., 2019), to connect synaptic effects to behavioral readouts. T-LTP was also reported to depend on brain-derived neurotrophic factor signaling (e.g., Edelmann et al., 2015; Lu et al., 2014; Mu and Poo, 2006; Pattwell et al., 2012; Sivakumaran et al., 2009). Still, these mechanistic studies on t-LTP employed STDP protocols depending typically on 25-100 repeats at ≤1 Hz that are unlikely to occur at synapses during memory formation *in vivo*. Therefore, in the present study we started out to determine the minimum number of repeats of coincident activation of pre- and postsynaptic neurons required for successful t-LTP induction. To this aim, we used low repeat variants of our recently described canonical (1:1 pairing: Edelmann and Lessmann, 2011) and burst STDP protocols (1:4 pairing: Edelmann et al., 2015; Solinas et al., 2019). Although, STDP protocols involving low repeat synaptic activation have been used previously to induce t-LTP (somatosensory cortex: Cui et al., 2015; Cui et al., 2016; visual cortex: Froemke et al., 2006; cultured hippocampal cells: Zhang et al., 2009), the underlying cellular mechanisms for its induction and expression remained elusive.

Our present study demonstrates, that Schaffer collateral (SC)- CA1 t-LTP can be induced robustly by only three to six repeats of coincident pre- and postsynaptic spiking at 0.5 Hz. Moreover, our study reveals that, depending on specific STDP paradigms (i.e. 1:1 vs. 1:4) the low repeat protocols recruit distinct sources for postsynaptic Ca^{2+} elevation during induction of t-LTP, are mediated by distinct pre- and postsynaptic expression mechanisms, and are differentially regulated by dopamine receptor signaling. Together these data suggest that hippocampal SC-CA1 synapses can recruit multiple types of synaptic plasticity in response to low repeat STDP protocols for processing of information and memory storage in the hippocampus. Altogether, these distinct cellular STDP pathways might form the basis for the pluripotency of hippocampal functions in learning and memory.

Results

Timing-dependent LTP at Schaffer collateral-CA1 synapses requires 3-6 spike pairings

Using whole cell patch clamp recordings, we investigated timing-dependent (t-)LTP at Schaffer collateral (SC) -CA1 synapses in acute hippocampal slices obtained from juvenile (i.e. P28-35) male C57BL/6J mice. T-LTP was induced by STDP protocols consisting of low repeat coincident pre- and postsynaptic action potentials at low pairing frequencies (0.5 Hz).

SC-CA1 synapses were repeatedly activated by pairing of an excitatory postsynaptic potential (EPSP) that was elicited by supra-threshold extracellular SC stimulation, with a single postsynaptically evoked action potential (AP; 1EPSP/1AP or 1:1, Δt= 10 ms at 0.5 Hz; compare **Fig 1A**). To determine the minimal repeat number required for successful t-LTP induction with a prototypical STDP paradigm, neurons were subjected to either 70, 25, 6, or 3 repeats of single spike pairings. Unexpectedly, we found that just six spike pairings with 1:1 stimulation delivered at a frequency of 0.5 Hz were sufficient to induce robust potentiation of EPSP slopes to 154.5% ± 8.2% at 30 min after induction. The t-LTP magnitude was similar to the respective magnitude of t-LTP induced with either 25 or 70 repeats and significantly different from negative controls (25 x: 145.4% ± 9.1% and 70 x: 166.9% ± 11.8; ANOVA $F_{(4,114)}$=4,8562 p=0.0012, STDP experiments performed with 3 x 1:1 stimulation at 0.5 Hz, showed only a very slight average increase of EPSP slopes to 104.6 ± 22.5% 30 min after induction that was highly variable between cells. The average value was not significantly different from the respective EPSP slopes observed after 40 min in control neurons that were not subjected to STDP stimulation (negative controls (0:0): 105.0% ± 6.5%; **Fig 1A**). The time course of changes in synaptic strength in an individual cell that was potentiated with the low repeat 1:1 protocol is depicted at the right side in blue. These data indicate that t-LTP can be induced at SC-CA1 synapses with low repeat t-LTP paradigms (i.e. 6 x 1:1), that might more closely resemble the natural pattern of pre- and postsynaptic activity that can be observed during memory formation in CA1 *in vivo* than any high frequency or high repeat LTP protocol.

Since it has been suggested, that successful induction of t-LTP at SC-CA1 synapses requires firing of multiple postsynaptic APs (Buchanan and Mellor, 2007; Pike et al., 1999; Remy and Spruston, 2007), we incorporated a postsynaptic burst (4 APs delivered at 200 Hz) into the 6 x 1:1 protocol (**Fig 1B**). This protocol is referred to as 6 x 1EPSP/4AP (or 6 x 1:4, **Fig 1B**) paradigm and induced t-LTP at SC-CA1 synapses with the same efficiency as the 6 x 1:1 protocol (compare **Fig 2C, D**). As for the canonical protocol, we determined the threshold number of repeats also for the burst protocol. As shown in figure 1B, successful 1:4 t-LTP could be induced by only three repeats of our burst protocol. Three, 6 and 35 repeats of 1:4 stimulation all yielded significant potentiation compared to the negative control (0 x repeats; ANOVA $F_{(4,42)}$=9.3654 p<0.0001, posthoc Dunnett's Test: 3 x: p=0.0017; 6 x: p<0.0001; 35 x: p=0.0415). The time course of change in synaptic strength of a typical cell obtained with 6 x 1:4 t-LTP stimulation is shown on the right. Since post-tetanic potentiation is lacking under these stimulation conditions, we observed for both t-LTP protocols a delayed onset (~5 min) and a subsequent gradual increase of t-LTP magnitude that typically proceeds until 30 min after induction, being consistent with previous t-LTP studies (compare e.g.,

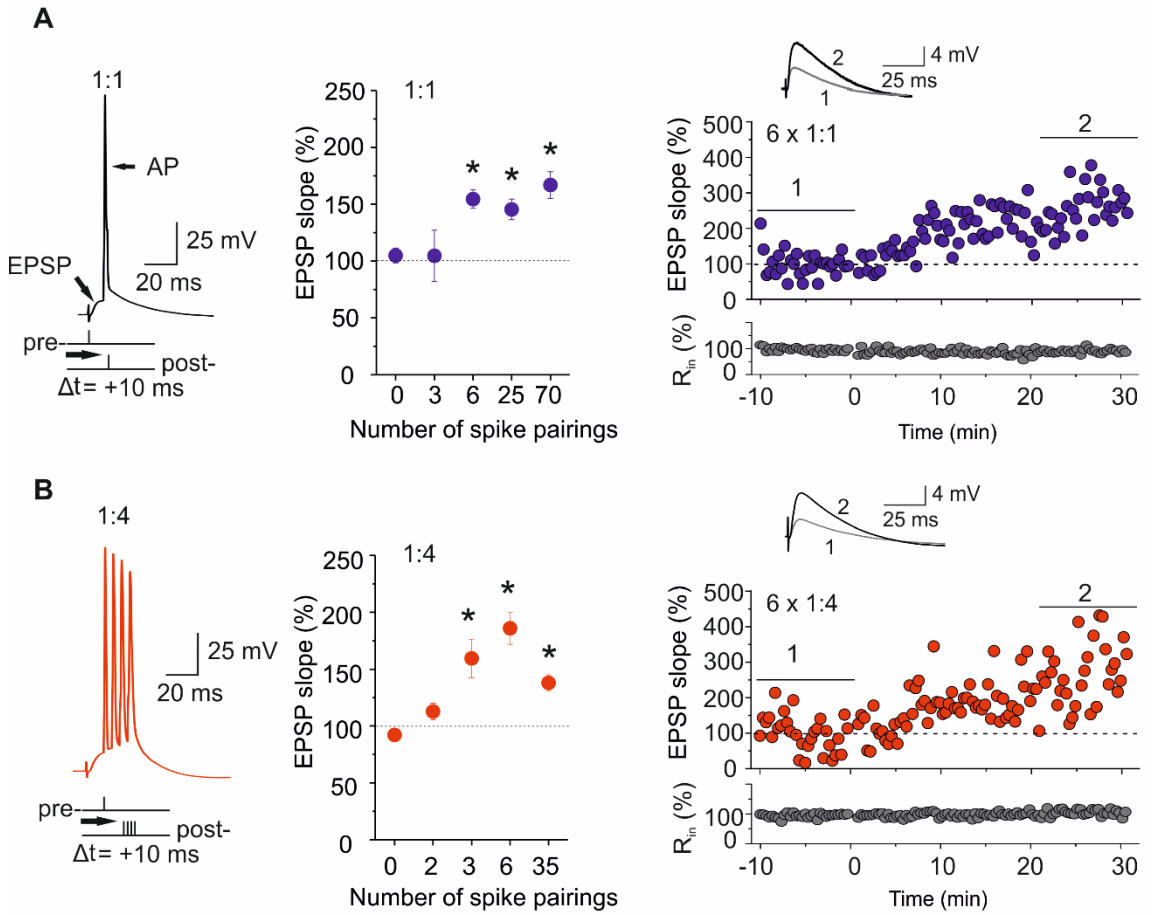

Figure 1: Low repeat t-LTP at Schaffer collateral-CA1 synapses is dependent on stimulation pattern and on the repeat number. A) *1:1 t-LTP protocol consisting of the temporal coincident stimulation of an EPSP and one postsynaptic action potential (AP) with a time delay of +10 ms. Summary plot showing the average magnitude of t-LTP (EPSP slope normalized to baseline recording) in response to variable numbers of repeats of the 1:1 t-LTP protocol delivered at 0.5 Hz. Successful t-LTP could be induced with 6 (n= 56 / N= 44), 25 (n= 25 / N= 6) and 70 (n=10 / N=7) repeats of the 1:1 t-LTP protocol. Three repeats did not cause any changes in synaptic strength (n=7 / N=6), and showed similar normalized EPSP slopes as negative controls (0:0; n=23 / N=17). Right: original EPSPs and time course of 6 x 1:1 induced potentiation recorded in an individual representative cell example of a single STDP experiment performed for 6x 1:1 stimulation.* ***B)*** *1:4 t-LTP protocol consisting of the temporal coincident stimulation of an EPSP and four postsynaptic action potentials (APs) with a time delay of +10 ms. Summary plot showing the average magnitude of t-LTP (EPSP slope normalized to baseline recording) in response to variable numbers of repeats of the 1:4 t-LTP protocol delivered at 0.5 Hz. Successful t-LTP could be induced with 3 (n=10 /N= 3), 6 (n=10 / N=6) and 35 (n=10 / N=8) repeats of the 1:4 t-LTP protocol. Two repeats did not cause changes in synaptic strength (n=10 /N =3) and showed similar normalized EPSP slopes as negative controls (0:0; n=8 / N=3). Right: original EPSPs and time course of 6 x 1:4 induced potentiation recorded in an individual representative cell. Averaged traces for EPSPs before and after LTP induction are shown as insets. * p < 0.05 ANOVA posthoc Dunnet's test. Data are shown as mean ± SEM.*

Banerjee et al., 2009; Edelmann et al., 2015; Edelmann and Lessmann, 2011; Meredith et al., 2003; Nevian and Sakmann, 2006; Pattwell et al., 2012).

For further comparison and analysis of signaling and expression mechanisms of t-LTP we focused in all subsequent experiments on the 6 repeat protocols that induced with the same number of repeats successful t-LTP for both, the canonical and the burst paradigm (indicated as 6 x 1:1 or 6 x 1:4).

Canonical and burst containing low-repeat STDP paradigms induce Hebbian t-LTP

When spike pairings were delivered with longer time delays between pre- and postsynaptic firing (Δt: +20 ms) the magnitude of t-LTP declined (6 x 1:1: 132.1% ± 17.5% and 6 x 1:4: 118.3% ± 9.8). Stimulation with short negative time delays (post-pre; Δt: -15 ms) did neither induce t-LTP nor significant t-LTD (6 x 1:1: 86.9% ± 9.6%; 6 x 1:4: 106.5 ± 10.5%; **Fig 2A, B**).

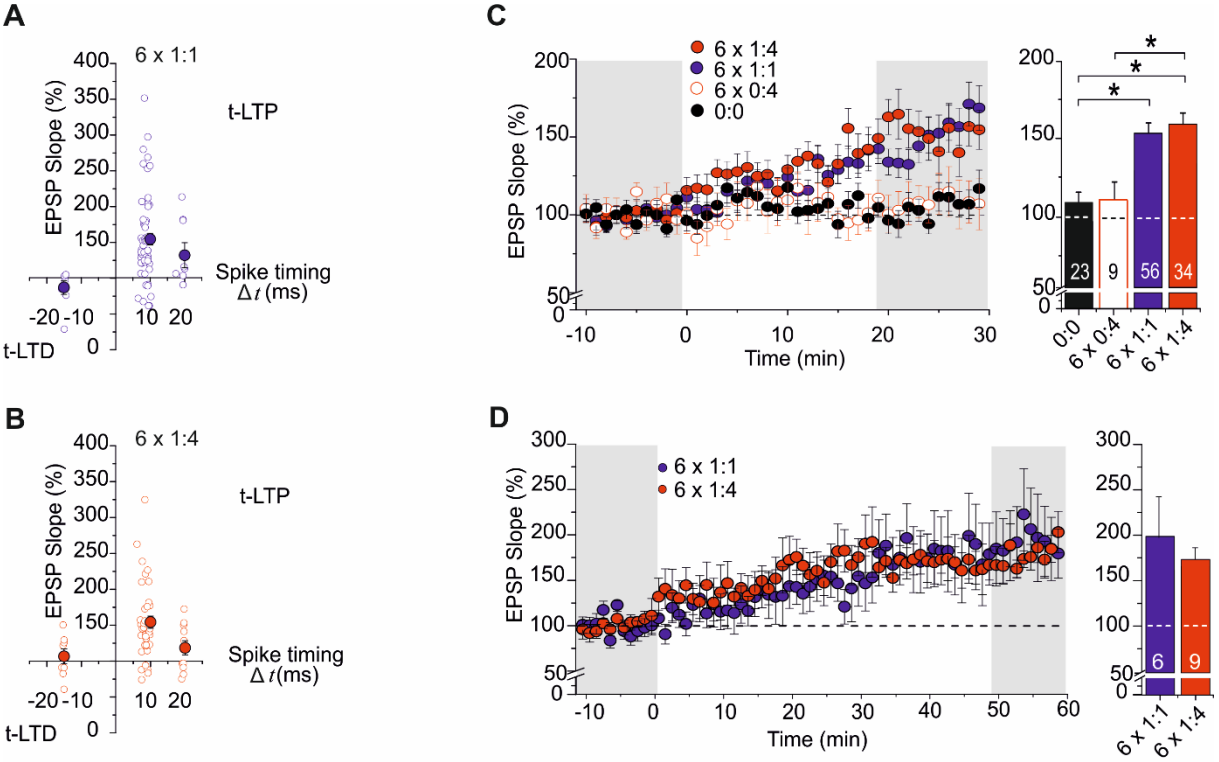

Figure 2: Comparison of canonical and burst low repeat STDP paradigms. *STDP plots for 6 x 1:1 (**A**, blue) and 6 x 1:4 (**B**, red) protocols. Changes in synaptic strength are shown for different intervals between start of the EPSP and postsynaptic APs. Groups of cells at +10 ms interval (standard), with longer time interval (+20 ms) or with negative spike pairings (-15 ms) are shown. Each open circle represents the result for an individual CA1 neuron. Mean values are shown as closed circles.* ***C)*** *The time courses of t-LTP expression do not differ between 6 x 1:1 (n= 56 / N= 44) and 6 x 1:4 (n= 34 / N= 27) paradigms, but they were significantly different from negative controls (0:0; n= 23 / N= 17) and unpaired controls (6 x 0:4; n= 9 / N= 7). The average magnitude of t-LTP is shown in the bar graphs.* ***D)*** *Extended measurements for 1 hour after t-LTP induction for both low repeat STDP protocols (6 x 1:1: n=6 / N=6, 6 x 1:4: n=9 / N=8). Data are shown as mean ± SEM, bar scales are shown in the insets.*

In general, the magnitude of t-LTP induced with the 6 x 1:4 stimulation (159.6% ± 8.0%) was comparable to that observed for 6 x 1:1 stimulation (154.5% ± 8.2%; p > 0.05, compare **Fig 2C**). Eliciting only postsynaptic bursts without pairing to presynaptic stimulation (6 x 0:4; 110.0 ± 11.9%) was not significantly different from negative controls (0:0; 108.6% ± 7.1%, p > 0.05; **Fig 2C**). Importantly, these results indicate that repeated postsynaptic burst firing alone does not induce any change in synaptic strength, indicating hebbian features for our low repeat t-LTP protocols thereby delineating our protocols from non-hebbian behavioral time scale synaptic plasticity recently reported for hippocampal places cells (Bittner et al., 2017). Prolonged patch clamp recordings carried out for 1 hour after pairing showed that both low repeat STDP paradigms yielded at 60 min comparable t-LTP magnitudes as observed 30 min after pairing. These data demonstrate that both low-repeat protocols enable longer lasting changes in synaptic

transmission without any decline in magnitude. Moreover, the overall time course of the potentiation was indistinguishable for both types of low repeat t-LTP (**Fig 2D**). Together, these findings indicate that the low repeat STDP paradigms identified in this study induce Hebbian plasticity selectively at short positive spike timings with similar properties as have been described in earlier studies using high repeat canonical and burst type STDP protocols (e.g., Bi and Poo, 1998; Edelmann et al., 2015; Froemke et al., 2006).

In the next series of experiments, we determined the mechanisms of induction and expression as well as the intracellular signaling cascades involved in modulation of both types of low repeat t-LTP.

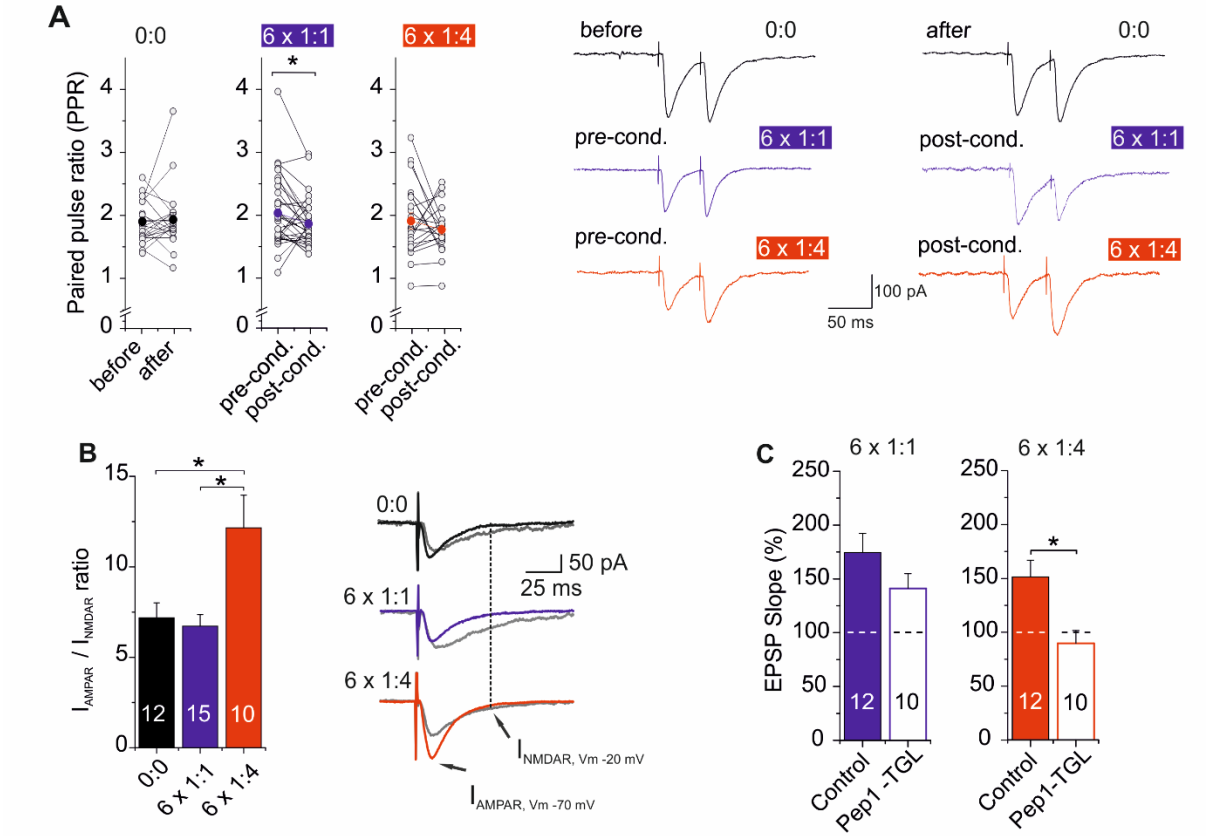

Figure 3: Different loci of expression for t-LTP induced by the low repeat 1:1 and 1:4 paradigms. A) *Paired pulse ratio (PPR) calculated before (pre-cond.) and 30 min after (post-cond.) t-LTP induction, or at the beginning and the end of measurements in negative controls (0:0: n=18/N= 16; 6 x 1:1: n=29/N= 24; 6 x 1:4: n=31/N=23 animals).* ***B)*** *Right: original traces of AMPAR mediated currents recorded in voltage clamp at -70 mV holding potential (Vm) and NMDAR (gray) mediated currents at -20 mV holding potential. Left: ratio of AMPA/NMDA receptor mediated currents (AMPAR: peak current at -70 mV; NMDAR: current amplitude 50 ms after start of EPSC, recorded at -20 mV) for negative controls (0:0; n=12 / N= 9) and after induction of t-LTP with both low repeat paradigms (6 x 1:1: n= 12 / N=11; 6 x 1:4: n= 7 / N= 5).* ***C)*** *Intracellular application of Pep1-TGL (inhibiting membrane insertion of GluA containing AMPARs) blocks 6 x 1:4 t-LTP, whereas 6 x 1:1 t-LTP remains intact (6 x 1:1: ACSF; n= 12 / N= 10, Pep1-TGL n= 9 / N= 7 and 6 x 1:4: ACSF n= 11 / N= 11, Pep-TGL n= 9 / N= 7). Data are shown as mean ± SEM. Scale bars are shown in the figures.*

Influence of single and multiple postsynaptic action potentials on t-LTP expression

To investigate whether the low repeat STDP paradigms introduced here, rely on pre- or postsynaptic expression mechanisms of synaptic plasticity, we determined changes in the paired pulse ratio (PPR) before and 30 min after t-LTP induction that was obtained when two successively evoked EPSPs were elicited at 50 ms inter-stimulus interval (**Fig 3A**). Commonly, a decrease in PPR after induction of LTP is interpreted as an increase in transmitter release probability and would be expected in case of

presynaptically expressed synaptic plasticity. When t-LTP was induced with the 6 x 1:1 paradigm we found on average in fact a significant decrease in PPR (paired Student's t-test, $t_{(34)}$ =2.3471; p= 0.0249, whereas the PPR remained unchanged after inducing 6 x 1:4 t-LTP (paired Student's t-test, $t_{(20)}$ = 1.0146; p = 0.3224; **Fig 3A**). This decreased PPR after induction of 6 x 1:1 t-LTP hints at a presynaptic expression mechanism. In contrast, the PPR analysis clearly speaks against any presynaptic contribution in the expression of 6 x 1:4 t-LTP. Interestingly, the initial PPR before inducing t-LTP was not significantly different between the tested groups (negative control (0:0): 1.77 ± 0.09; 6 x 1:1: 1.78 ± 0.08; 6 x 1:4: 1.74 ± 0.06; Kruskal-Wallis test, $H_{(2)}$ = 0.059; p = 0.9710), indicating that the initial release probability was similar and a stable basal parameter in our slices. As additional measures for a presynaptic expression mechanism, we determined miniature EPSCs and coefficient of variation (CV) analysis before and after successful induction of our 6x 1:1 t-LTP (Fig S1, compare Bender et al., 2009; Edelmann et al., 2015). The results of both types of analysis are consistent with presynaptic expression of 6 x 1:1 t-LTP, as the overall mean for CV after LTP was decreased, and miniature EPSC frequencies (determined as shorter inter event intervals (IEI)) were increased after 6 x 1:1 t-LTP induction (see **Fig S1**).

To further address the locus of expression of 6 x 1:1 and 6 x 1:4 t-LTP, we analyzed the changes in AMPA/NMDA receptor (R) mediated current ratios 30 min after inducing t-LTP. AMPAR mediated peak EPSCs were recorded at a holding potential of -70 mV, while NMDAR mediated current components were determined as remaining current 50 ms after the peak EPSC recorded at -20 mV to avoid large current fluctuations of holding currents that are typically observed at positive membrane potentials. The AMPA/NMDA ratio analysis revealed a strong and statistically significant increase in AMPAR- vs. NMDAR-mediated excitatory postsynaptic currents (EPSCs) following the induction of 6 x 1:4 t-LTP but not when inducing 6 x 1:1 t-LTP, or in non-STDP stimulated control cells (ANOVA $F_{(2, 34)}$ = 7.979; p = 0.0014, **Fig 3B**). Since recording of NMDAR mediated currents at -20 mV (instead of +40 mV) results in smaller current amplitudes we might have introduced a larger error. However, since all groups (negative control, 6 x 1:1 and 6 x 1:4) were handled identically in this respect, the significant change specifically after t-LTP induction with 6 x 1:4 protocol, clearly points to a strong increase of postsynaptic AMPAR conductance, which is absent in the other groups. Since an increase in AMPAR/NMDAR mediated currents after inducing LTP is commonly explained by the insertion of new GluA1 containing AMPARs into the postsynaptic spine (Chater and Goda, 2014; Edelmann et al., 2015; Lee and Kirkwood, 2011; Morita et al., 2014) these data strongly suggest a postsynaptic mechanism of expression selectively for the 6 x 1:4 t-LTP. Nevertheless, the AMPAR/NMDAR ratio can also be increased by postsynaptic mechanisms other than AMPAR receptor insertion (such as e.g. phosphorylation). Thus, we next investigated whether the 6 x 1:4 t-LTP is mediated specifically by incorporation of GluA1 containing AMPARs. To this aim, we loaded the postsynaptic cells with Pep1-TGL via the patch pipette solution and induced t-LTP with both 6 repeat t-LTP paradigms (compare Edelmann et al., 2015). Pep1-TGL contains the last three amino acids of the C-terminus of the GluA1 subunit, which are required for its insertion into the plasma membrane (Hayashi et al., 2000; Shi et al., 2001). The postsynaptic application of Pep1-TGL resulted in a complete block of 6 x 1:4 t-LTP (Mann-Whitney U test, U = 14.0; p = 0.007). In contrast, t-LTP induced with the 6 x 1:1 protocol remained intact under the same recording conditions (Mann-Whitney U test, U = 36.0; p =0.201, **Fig 3C**). Together with the PPR analysis and the AMPA/NMDAR ratios, these data suggest a dominant postsynaptic locus of expression for the 6 x 1:4 t-LTP. In contrast, the absence of any change in AMPA/NMDAR current ratio and AMPAR insertion, in conjunction with the decreased PPR, decreased CV (paired student's t-test: $t_{(48)}$=4.5874; p< 0.0001), and increased mEPSC frequency (Kolmogorov-Smirnov 2sample test: Z=1.5745, p= 0.0132; compare **Fig S1**) indicate a prevailing presynaptic locus of expression for the 6 x 1:1 t-LTP. These findings are consistent with our previous results obtained with high repeat t-LTP protocols (Edelmann et al., 2015). The data suggest that the number of postsynaptic spikes fired during induction of low repeat t-LTP decides whether associative Hebbian synaptic plasticity is expressed by pre- or by postsynaptic mechanisms, whereas the locus of t-LTP expression does not seem to depend on the number of repeats of a specific t-LTP paradigm.

Distinct calcium sources are recruited for induction of low repeat STDP paradigms

There is a general consensus that induction of long-lasting changes in synaptic strength at SC-CA1 synapses requires a postsynaptic rise in intracellular calcium concentration ($[Ca^{2+}]_i$) via NMDA receptors (NMDARs, Nicoll and Malenka, 1995). Likewise, also intracellular Ca^{2+} elevation resulting from synchronous activation of NMDARs, L-type voltage-gated Ca^{2+} channels (VGCC), and release of Ca^{2+} from internal stores, together with activation of metabotropic glutamate receptors (mGluRs) and subsequent activation of IP_3 receptors might be responsible for postsynaptic STDP induction (Tigaret et al., 2016). Accordingly, we investigated the sources for the intracellular Ca^{2+} elevation triggering the 6 x 1:1 and 1:4 t-LTP. Interestingly, the 6 x 1:1 t-LTP was significantly impaired when it was executed either in the presence of the specific NMDAR antagonist APV (50 µM; unpaired Student's t-test, $t_{(26)} = 2.348$; $p = 0.0268$; **Fig 4A**), or in the presence of the L-type VGCC blocker Nifedipine (25 µM; unpaired Student's t-test, $t_{(14)} = 4.25$; $p = 0.0008$; **Fig 4C**). In contrast, neither APV (50 µM, unpaired Student's t-test, $t_{(22)} = 1.016$; $p = 0.3207$; **Fig 4B**) nor Nifedipine (25 µM, Mann-Whitney U test, $U = 20.0$; $p = 0.6620$, **Fig 4D**) inhibited t-LTP induced with the 6 x 1:4 protocol. These data indicate that postsynaptic Ca^{2+} influx via NMDAR and L-type VGCC is required for 6 x 1:1 t-LTP but not for 6 x 1:4 t-LTP induction.

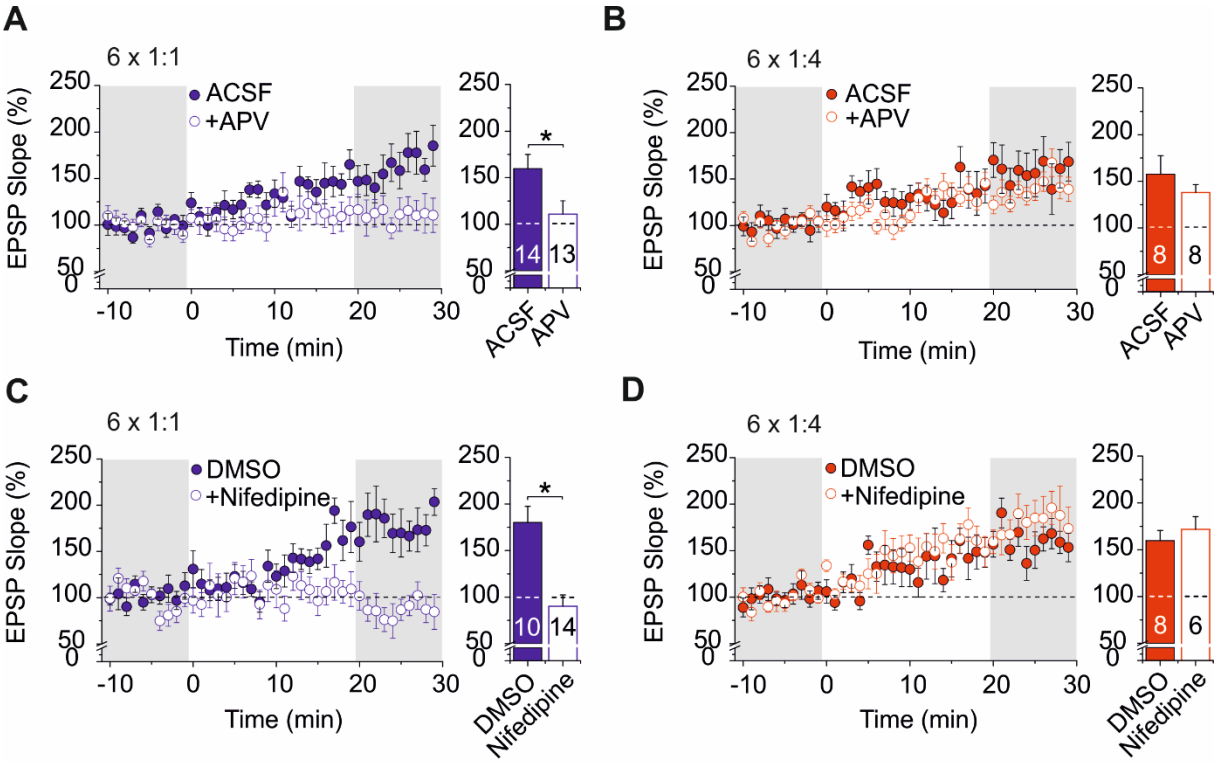

Figure 4: Contribution of NMDA receptors and VGCCs to the induction of 6 x 1:1 and 6 x 1:4 t-LTP. *Effects of bath applied NMDAR antagonist APV (50 µM) and L-type voltage-gated calcium channel (VGCC) inhibitor Nifedipine (25 µM) on low repeat t-LTP. Inhibition of either NMDARs* ***(A)*** *or L-type VGCCs* ***(C)*** *completely blocked 6 x 1:1 t-LTP (A: 6 x 1:1: ACSF n=14 / N=8, APV n= 13 / N= 12; C: DMSO control n= 8 / N=7, Nifedipine n=8 / N=7).* ***(B)*** *6 x 1:4 t-LTP remained unaffected by application of the NMDAR inhibitor APV (6 x 1:4: ACSF n=10 / N=6, APV n=14 / N=9).* ***D)*** *6 x 1:4 t-LTP was not inhibited in the presence of the L-type VGCC inhibitor nifedipine (DMSO n=8 / N=4, Nifedipine n=6 / N=4). Average time course of potentiation and mean (± SEM) magnitude of t-LTP are shown for the respective experiments.*

To verify a role of postsynaptic Ca^{2+} signaling in the induction of 6 x 1:4 t-LTP, we loaded postsynaptic neurons with 10 mM of the Ca^{2+} chelator BAPTA via the patch pipette solution (**Fig 5A**). After obtaining the whole cell configuration, the BAPTA containing internal solution was allowed to equilibrate for 30 min before t-LTP induction. Likewise, in the respective control experiments t-LTP was also induced 30 min

after breaking the seal. As shown in **figure 5A**, buffering of intracellular Ca^{2+} signals with BAPTA resulted in a complete impairment of 6 x 1:4 t-LTP (Mann-Whitney U test, U = 3.0; p =0.0303), indicating that a rise in postsynaptic $[Ca^{2+}]_i$ is indeed required also for the induction of 6 x 1:4 t-LTP.

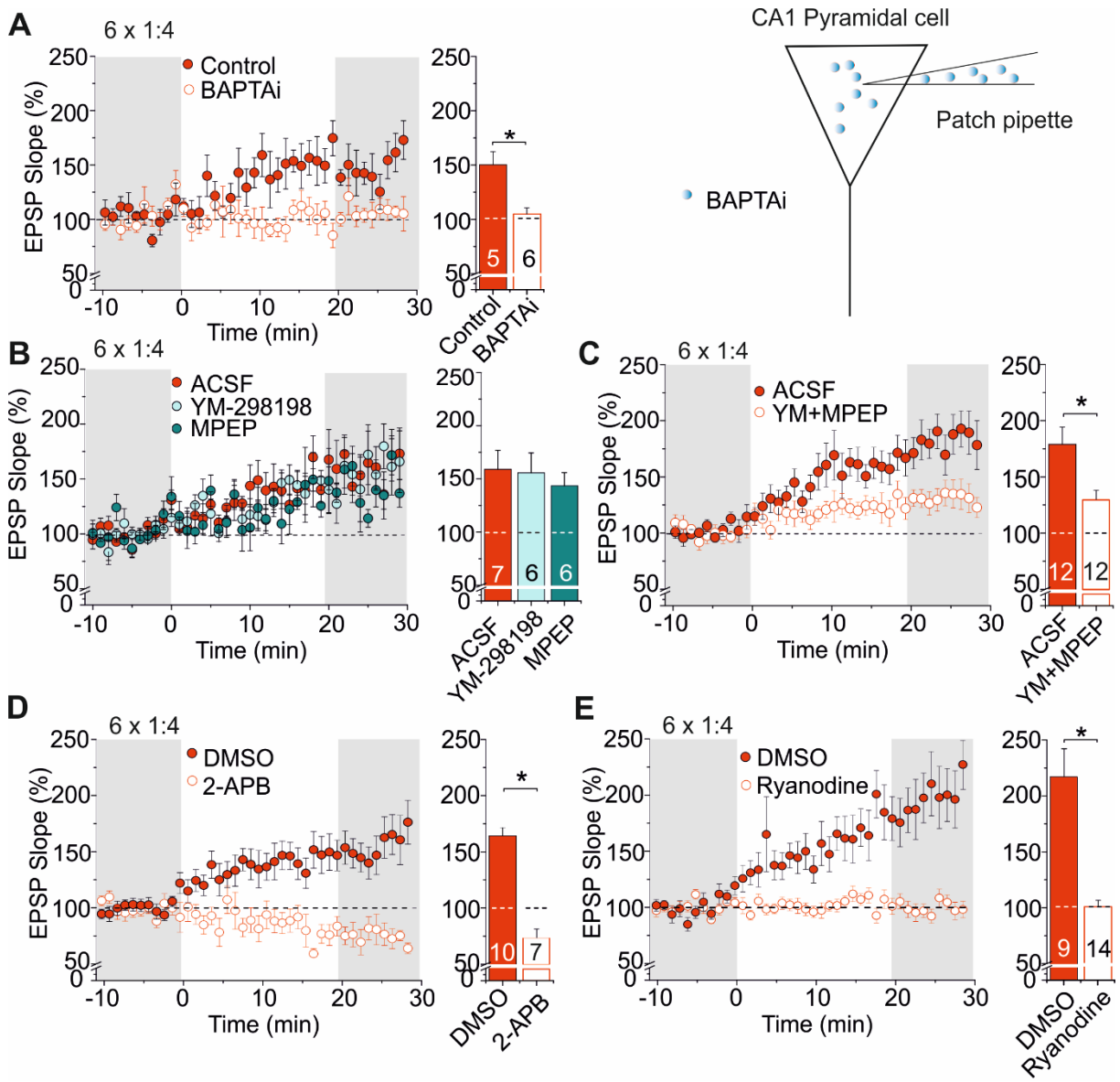

Figure 5: Contribution of group I mGluRs, IP3 receptors and ryanodine receptor-dependent calcium release from internal stores to 6 x 1:4 t-LTP. A) *Inclusion of 10 mM BAPTA in the pipette solution and equilibration with the cell interior for 30 min before t-LTP induction (open circles) prevented t-LTP induced by 6 x 1:4 stimulation compared to identically treated (i.e. t-LTP induction 30 min after breaking the patch) control cells (closed circles; Control: n=5 / N=5, BAPTA$_i$: n=6 / N=4), indicating the necessity of postsynaptic calcium elevation to induce t-LTP. The inset depicts the loading of the cell with BAPTA.* ***B)*** *T-LTP induced with the 6 x 1:4 protocol was neither affected by bath application of the mGluR1 antagonist YM-298198 (1 µM; ACSF: n=7 / N=5, YM-298198: n=6 / N=3), nor by the mGluR5 antagonist MPEP (10 µM, n=6 / N=4).* ***C)*** *However, co-application of both antagonists (YM-298198 and MPEP; ACSF n=12 / N=8, YM-MPEP n=12 / N=5) significantly reduced synaptic potentiation.* ***D)*** *Inhibition of IP3 receptors by 100 µM 2-APB (in 0.05% DMSO) completely blocked 6 x 1:4 t-LTP (DMSO n = 10/ N = 5; 2-APB n = 7/ N =3).* ***E)*** *Wash in of 100 µM ryanodine into the postsynaptic neuron via the patch pipette inhibited t-LTP induced by 6 x 1:4 stimulation (DMSO n= 9 / N= 4; Ryanodine n= 14 / N= 5). Average time course of potentiation and mean (± SEM) magnitude of t-LTP are shown for the respective experiments.*

Since induction of t-LTP involves repeated glutamate release that, according to hebbian rules, should contribute to the induction process, we next tested the involvement of metabotropic glutamate receptors (mGluRs) in 6 x 1:4 t-LTP. In the hippocampal CA1 region $mGluR_1$ and $mGluR_5$ are widely expressed and have been reported to facilitate Ca^{2+} release from internal calcium stores during LTP (e.g., Balschun et al., 1999; Neyman and Manahan-Vaughan, 2008; Wang et al., 2016). Nevertheless, blocking mGluR activation by bath application of antagonists of either $mGluR_1$ (YM198298, 10 µM) or $mGluR_5$ (MPEP, 10 µM) alone, did not affect the magnitude of 6 x 1:4 t-LTP compared to ACSF controls (Kruskal-Wallis test, $H_{(2)} = 0.2774$; $p = 0.8705$; **Fig 5B**). However, coapplication of the $mGluR_1$ and $mGluR_5$ antagonists significantly reduced the 6 x 1:4 t-LTP magnitude (unpaired Student's t-test, $t_{(22)} = 2.248$; $p = 0.0093$; **Fig 5C**), indicating that the activation of one of these receptors alone (either $mGluR_1$ or $mGluR_5$) is sufficient and required to support 6 x 1:4 t-LTP. To investigate whether mGluR mediated Ca^{2+} release from internal stores contributes to 6 x 1:4 t-LTP we used 2-APB as an inhibitor of IP_3-receptors. As expected inhibition of IP_3-mediated Ca^{2+} release completely blocked t-LTP (unpaired Student's t-test, $t_{(15)}=4.0297$; $p = 0.0019$, **Fig 5D**).

To test for involvement of ER-resident ryanodine receptors (RyR) in the low repeat burst protocol, we applied 100 µM ryanodine (a concentration known to irreversibly inhibit RyR; Gao et al., 2005) via the patch pipette into the recorded postsynaptic neurons. As expected in case of RyR involvement, 6 x 1:4 t-LTP induction was completely inhibited under these conditions (Mann-Whitney U test, $U= 5.5$; $p = 0.0003$; Fig 5D). These data indicate that Ca^{2+} release from the ER is a critical component of 6 x 1:4 t-LTP. Thus, the postsynaptic Ca^{2+} elevation required for induction of 6 x 1:4 t-LTP seems to involve $mGluR_1$ or $mGluR_5$ mediated release of Ca^{2+} from the ER via IP3 receptors and subsequent Ca^{2+} induced Ca^{2+} release via RyRs.

Distinct dopaminergic modulation of different low repeat t-LTP protocols at Schaffer collateral-CA1 synapses

Dopamine (DA) serves as an important neuromodulator in learning and memory formation, as well in synaptic plasticity mechanisms underlying both phenomena. DA receptors in the brain are classified into two main families: D1-like receptors that include D1 and D5, and D2-like receptors that include D2, D3 and D4 (Missale et al., 1998). It has been shown that activation of D1/D5 receptors has a particularly strong influence on synaptic efficacy (e.g., Dubovyk and Manahan-Vaughan, 2018; Papaleonidopoulos et al., 2018), and that treatment of cultured hippocampal neurons with exogenous DA (20 µM) reduces the induction threshold for t-LTP from 60 to 10 spike pairings (Zhang et al., 2009). To examine whether in our case, endogenous DA signaling is an essential component of synaptic mechanisms triggering low repeat t-LTP, we investigated the effect of specific bath applied antagonists for D1-like and D2-like DA receptors (D1: SCH23390 (SCH), 10 µM; D2: Sulpiride (Sulp), 10 µM). We found that t-LTP induced with 6 x 1:1 stimulation was blocked completely when SCH23390 and Sulpiride were coapplied (Kruskal-Wallis test, $H_{(3)} = 14.28$; $p = 0.003$), whereas application of either the D1-like or the D2-like receptor antagonist alone did not significantly reduce the magnitude of the 6 x 1:1 t-LTP (Fig 6A). In contrast, the 6 x 1:4 t-LTP was dependent exclusively on D2-like receptor signaling, as was evident from complete inhibition of this burst t-LTP in the presence of Sulpiride (significantly different from ACSF controls; Kruskal-Wallis test $H_{(3)} = 12.65$; $p = 0.005$, Fig 6B), whereas SCH23390 was without effect.

Together, these data indicate that 6 x 1:1 t-LTP depends on D1/D2 receptor co-signaling whereas 6 x 1:4 t-LTP is only dependent on D2 receptors, highlighting a novel and important role of D2 receptors in both types of t-LTP. This is at variance with the fact that most previous studies investigating DA-dependent conventional LTP at SC-CA1 synapses reported an eminent role of D1-like receptors in high frequency induced LTP forms (e.g., Hagena and Manahan-Vaughan, 2016; Papaleonidopoulos et al., 2018). However, our results are fully consistent with the recently described D2 receptor mediated enhancement of t-LTP in the prefrontal cortex (Xu and Yao, 2010), and the prominent role of D2 receptors in hippocampus-dependent learning (Nyberg et al., 2016). A classical role for D1 receptor signaling was also described for for high repeat (70 x) canonical t-LTP in rat hippocampal slices (Edelmann and Lessmann, 2011, 2013). To

clarify whether repeat number or species matter for the contribution of D1 and D2 receptors in t-LTP, we examined DA dependence of high repeat 70 x 1:1 t-LTP in mouse hippocampal slices. We found that also in mouse slices 70 x 1:1 t-LTP was fully blocked by bath application of the D1 antagonist SCH23390 (unpaired Student's t-test, $t_{(22)} = 3.028$; p= 0.0062; **Fig 6C**). These data reveal that high repeat number induced t-LTP is regulated by D1 signaling whereas D2 signaling is selectively involved in low repeat t-LTP. Further, the extent of D2 receptor involvement in low repeat t-LTP is regulated by the postsynaptic spike pattern used for t-LTP induction (compare **Fig 6A** and **B**).

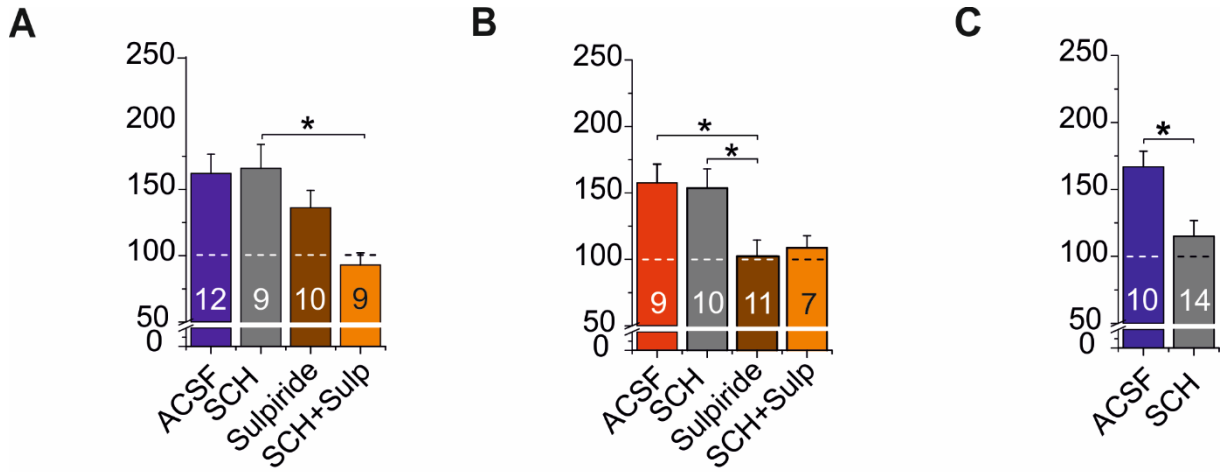

Figure 6: Differential modulation of canonical and burst low repeat t-LTP by dopaminergic signaling. A) *Dependence of 6 x 1:1 t-LTP on D1 and D2 receptor signaling. Neither bath application of SCH23390 (SCH, D1-like antagonist; 10 µM) nor bath application of Sulpiride (Sulp, D2-like antagonist; 10 µM) alone impaired t-LTP (ACSF: n=12 / N=9; SCH23390 n=9 / N=6; Sulpiride n=10 / N=8). However, co-application of both antagonists significantly reduced t-LTP (SCH + Sulp n=9 / N=4).* ***B)*** *T-LTP induced with the 6 x 1:4 protocol was impaired in the presence of Sulpiride, but not further reduced by co-application with SCH23390. Accordingly, application of SCH23390 alone did not affect 6 x 1:4 t-LTP (ACSF: n=9 / N=6; SCH23390 n=10 / N=5; Sulpiride n=11 / N=8; SCH + Sulp n=7 / N=4).* ***C)*** *T-LTP induced with the high repeat (70 x) 1:1 protocol was inhibited in the presence of the D1 receptor antagonist SCH23390 (10 µM) in mouse slices (ACSF n=10 / N=8; SCH23390 n=14 / N=5) to a similar extent as observed previously in rat hippocampal slices (Edelmann and Lessmann, 2011). Mean (± SEM) magnitude of t-LTP are shown for the respective experiments.*

The role of BDNF/TrkB signaling in low repeat t-LTP induced by canonical or burst protocols

We recently showed for SC-CA1 synapses that brain-derived neurotrophic factor (BDNF) induced tropomyosin related kinase B (TrkB) signaling mediates t-LTP elicited by a 1:4 t-LTP paradigm with 25 repeats at 0.5 Hz. This t-LTP is driven by an autocrine postsynaptic BDNF/TrkB mechanism that ultimately relies on postsynaptic insertion of new AMPA receptors (Edelmann et al., 2015). To address whether release of endogenous BDNF might be involved also in low repeat t-LTP, we next tested our low repeat t-LTP protocols in slices obtained from heterozygous BDNF knockout ($BDNF^{+/-}$) mice which express ~50% of BDNF protein levels compared to WT littermates (e.g., Endres and Lessmann, 2012; Psotta et al., 2015). Our results show that both types of low repeat t-LTP remained functional in response to this chronic depletion of BDNF (6 x 1:1 t-LTP: Mann-Whitney U test, U = 25.0; p = 0.7789; and 6 x 1:4 t-LTP: Mann-Whitney U test, U = 14.0; p = 0.5887, **Fig 7A**). Next, to examine whether acute inhibition of BDNF/TrkB signaling affects low repeat t-LTP, we asked whether scavenging of BDNF by bath applied TrkB receptor bodies (human TrkB-Fc chimera, TrkB-Fc) impairs low repeat canonical or burst t-LTP. However scavenging of BDNF had no effect on the magnitude of t-LTP induced by either of the two protocols (6 x 1:1 t-LTP: Mann-Whitney U test, U = 13.0; p = 0.0939 and 6 x 1:4 t-LTP: Mann-Whitney U test, U = 22.0; p = 0.8048, **Fig 7B**).

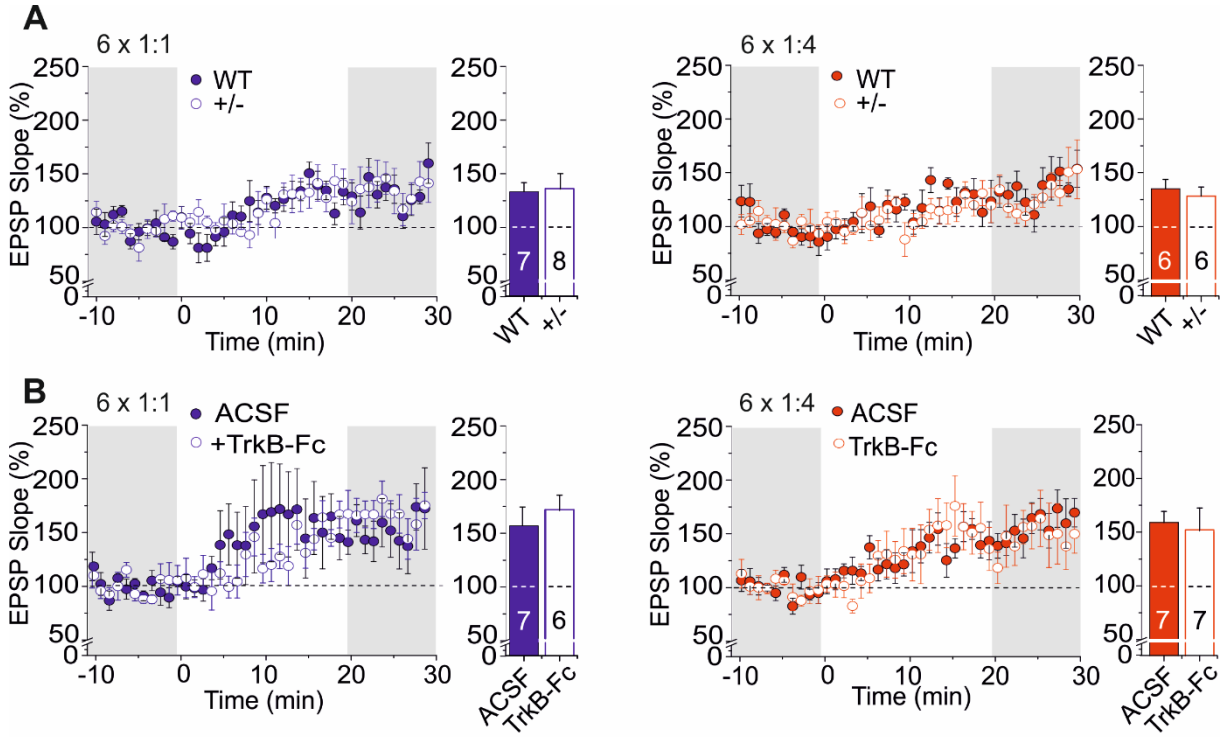

Figure 7: BDNF induced TrkB receptor signaling is not required for t-LTP elicited by low repeat t-LTP protocols. A) *Low repeat t-LTP was not different for 6 x 1:1 (left) and 6 x 1:4 (right) stimulation in heterozygous BDNF knockout animals ($^{+/-}$) compared to wild type litter mates (6 x 1:1: +/+ n 7 / N=6, +/- n=8 / N=7; 6 x 1:4: +/+ n=6 / N=5, +/- n=6 / N=5).* ***B)*** *Bath application of the BDNF scavenger TrkB-Fc (100 ng/ml; 3h preincubation) did not affect t-LTP in response to the two low repeat protocols (left: 6 x 1:1: ACSF n=7 / N=5, TrkB-Fc n=6 / N=6; right: 6 x 1:4: ACSF n=7 / N=5, TrkB-Fc n= 7 / N= 6). Average time course of potentiation and mean (± SEM) magnitude of t-LTP are shown for the respective experiments.*

Together these data suggest that 6 x 1:4 and 6 x 1:1 t-LTP are both independent from activity-dependent release of endogenous BDNF and downstream TrkB signaling. In conjunction with our previous observation that 25 x 1:4 t-LTP is dependent on release of endogenous BDNF (compare Edelmann et al., 2015) the present data suggest that a higher number (>6) of postsynaptic spike bursts in the t-LTP protocol is required to activate BDNF secretion.

The role of GluA2-lacking, calcium-permeable AMPA receptors in low repeat t-LTP

The transient incorporation of GluA2-lacking, Ca^{2+} permeable (cp-) AMPARs after LTP induction has been proposed as an important process to increase postsynaptic Ca^{2+} levels for LTP expression (Kauer and Malenka, 2006; Man, 2011; reviewed in Park et al., 2018; Plant et al., 2006). To examine whether these receptors are involved in low repeat t-LTP, we incubated our recorded hippocampal slices with the selective cp-AMPAR inhibitor NASPM (100 µM). Interestingly, 6 x 1:1 t-LTP and 6 x 1:4 t-LTP were both completely blocked in the presence of NASPM (6 x 1:1: unpaired Student's t-test, $t_{(14)} = 3.3502$; p= 0.0048; 6 x 1:4: unpaired Student's t-test, $t_{(19)} = 4.829$; p= 0.0002, **Fig 8A, B**). Surprisingly, these results indicate that the influx of Ca^{2+} via GluA2-lacking, cp-AMPARs is mandatory to elicit low-repeat t-LTP induction.

To rule out off-target effects of NASPM, we verified cp-AMPAR contribution in low repeat t-LTP with a second inhibitor of cp-AMPARs (IEM-1460, 100 µM). As shown in Figure 8C and D, we observed a comparable strong inhibition of low repeat t-LTP by IEM for both protocols (6 x 1:1: unpaired Student's t-test, $t_{(12)} = 2.76256$; p= 0.0172; 6 x 1:4: unpaired Student's t-test, $t_{(12)} = 4.4567$; p= 0.0007, **Fig 8C, D**).

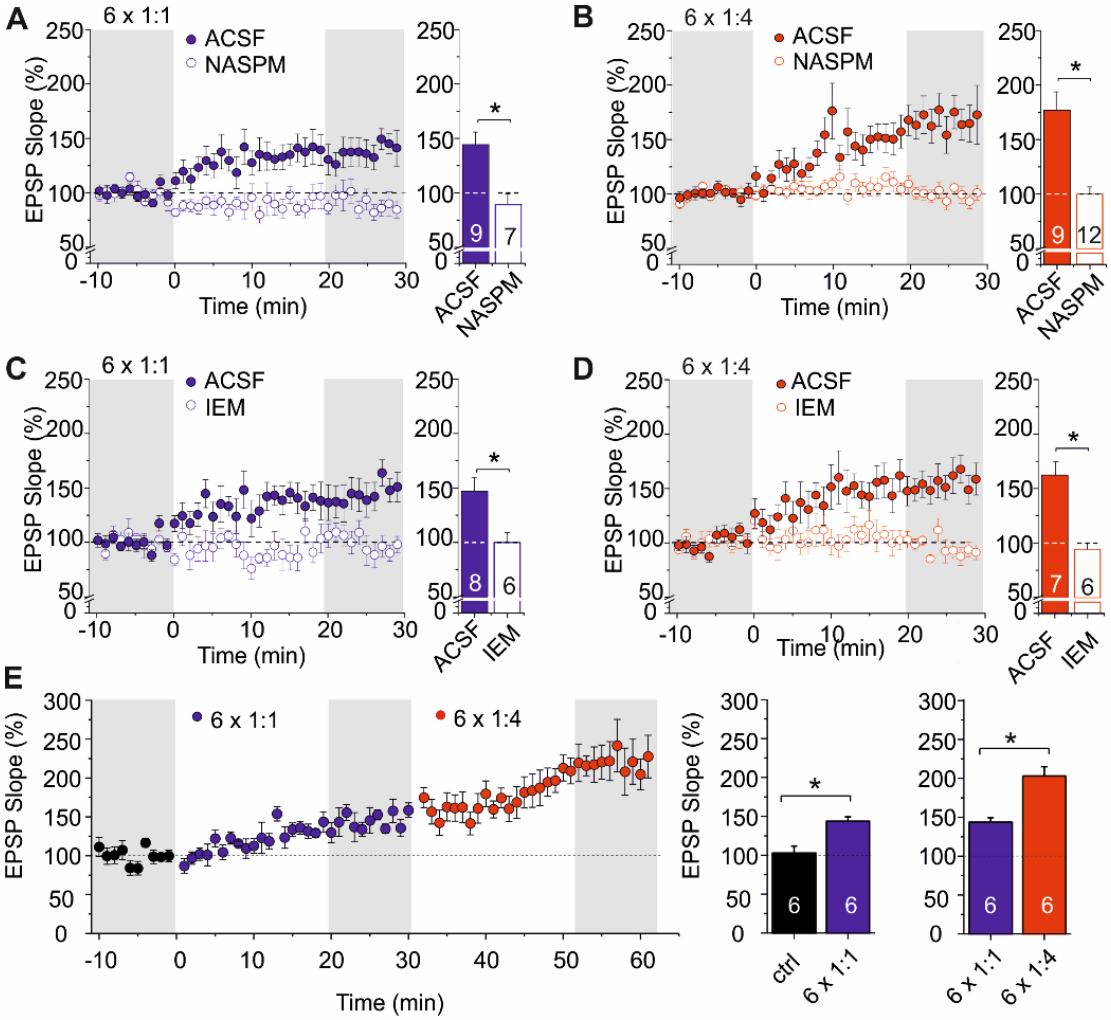

Figure 8: Ca^{2+} influx via GluA2-lacking calcium-permeable AMPARs is required for low-repeat t-LTP induction. *Bath application of a selective inhibitor of Ca^{2+} permeable AMPARs (100 µM NASPM) blocks 6 x 1:1 t-LTP (**A,** 6 x 1:1: ACSF n=9 / N=5, NASPM n=7 / N=3) as well as 6 x 1:4 t-LTP (**B**, 6 x 1:4: ACSF n= 9 / N=6 NASPM n=12 / N=5). Also IEM-1460 (100 µM), a second specific inhibitor of cp-AMPARs, blocks 6 x 1:1 t-LTP (**C,** 6 x 1:1: ACSF n=8 / N=5, IEM-1460 n=6 / N=3) as well as 6 x 1:4 t-LTP (**D**, 6 x 1:4: ACSF n= 8 / N=5, IEM n=6 / N=3). **E)** Successful induction of 6 x 1:1 t-LTP and subsequent 6 x 1:4 t-LTP in the same cells (n=6 / N=3). Note the absence of any signs of occlusion between t-LTP induced by the two low repeat protocols (compare **Fig S2**). Average time course of potentiation and mean (± SEM) magnitude of t-LTP are shown for the respective experiments*

In light of the many differences in the induction, expression mechanisms, and dopaminergic modulation of the canonical 6 x 1:1 t-LTP and the 6 x 1:4 burst t-LTP we asked whether both types of t-LTP can be elicited completely independent from one another or if they occlude each other. To this aim, we first induced 6 x 1:1 t-LTP followed in the same cells by a subsequently induced 6 x 1:4 t-LTP. As shown in **figure 8C**, both types of t-LTP could be activated independently without any signs of occlusion (1st t-LTP induction (6 x 1:1): $t_{(5)}$=-3.4618; p= 0.0180; 2nd t-LTP- induction (6 x 1:4): $t_{(5)}$=-4.7081; p= 0.0053, paired Student's t-test). Importantly, in another set of cells, subsequent stimulation for a second time with the same 6 x 1:1 protocol that had already successfully induced t-LTP, did not yield further potentiation (**Fig S2**; 1st t-LTP induction (6 x 1:1): $t_{(4)}$=-3.4607; p= 0.0258; 2nd t-LTP- induction (6 x 1:1): $t_{(4)}$=-1.9649; p= 0.1209; paired Student's t-test). Given the strong differences in the induction processes and the presynaptic expression of 6 x 1:1 vs. postsynaptic expression of 6 x 1:4 t-LTP, the absence of occlusion between the two protocols was an expected finding. However, this result corroborates the independence of the two different types of low repeat t-LTP investigated here.

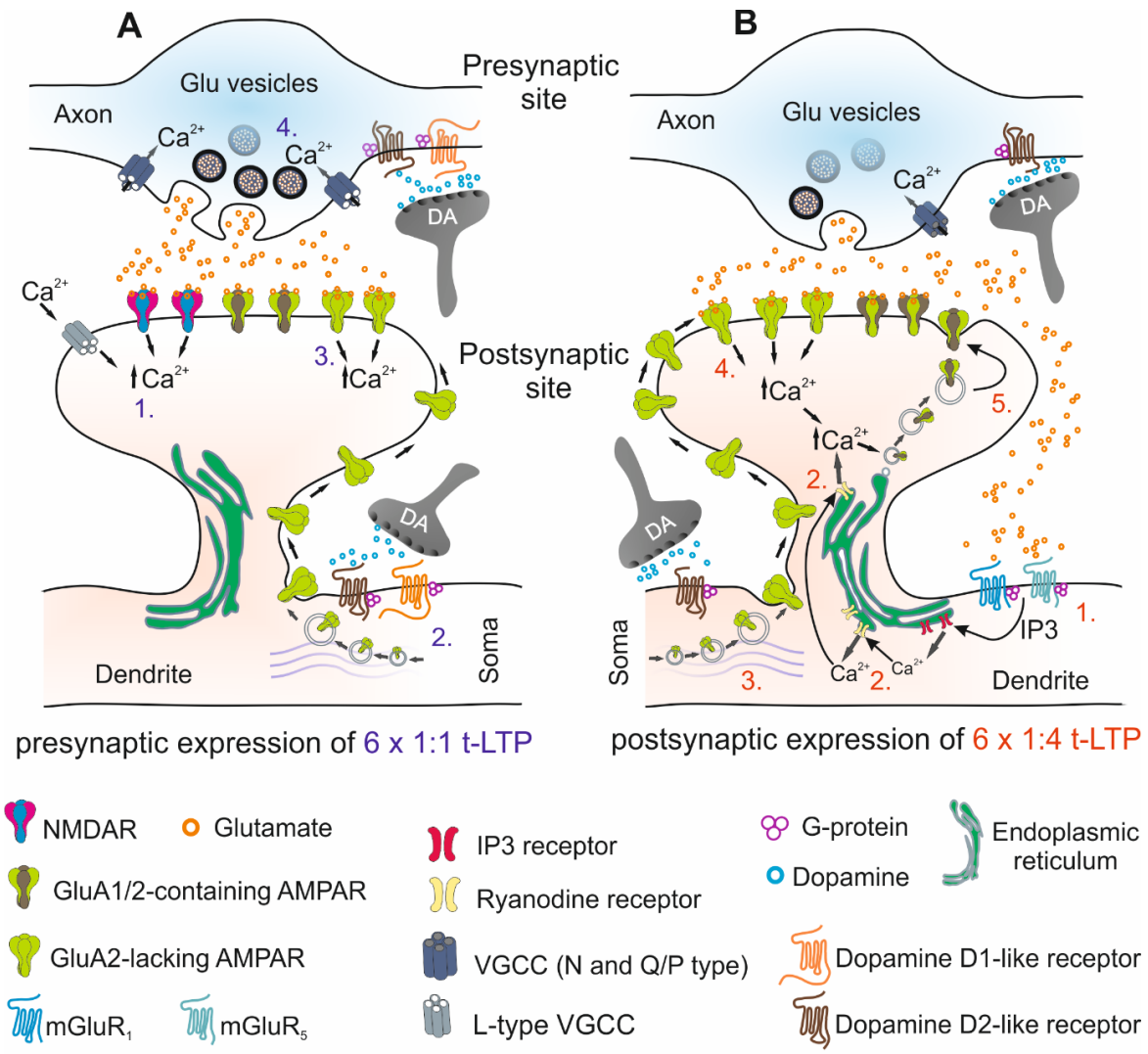

Figure 9: Suggested cellular signaling mechanisms involved in low repeat t-LTP at Schaffer collateral-CA1 synapses. *Summary of induction, signaling, and expression mechanisms involved in low repeat canonical (i.e. 6 x 1:1 t-LTP) and burst (i.e. 6 x 1:4) t-LTP protocols in CA1 pyramidal neurons.* ***A)*** *Synaptic mechanisms involved in the presynaptically expressed 6 x 1:1 t-LTP. T-LTP induction depends on postsynaptic NMDAR and L-type VGCC mediated Ca^{2+} influx (1.). Insertion of cp-AMPARs into the postsynaptic membrane might be regulated by D1/D2 signaling (2.) and could account for the combined D1/D2 receptor dependence of 6 x 1:1 t-LTP. Ongoing low frequency test stimulation after induction of t-LTP leads to sustained Ca^{2+} elevations through postsynaptic cp-AMPARs (3.). The resulting prolonged postsynaptic Ca^{2+} elevation leads via a yet unidentified retrograde messenger to increased presynaptic efficacy (4.). An additional presynaptic contribution of D1/D2 signaling to enhanced presynaptic glutamatergic function is possible.* ***B)*** *The postsynaptically expressed 6 x 1:4 t-LTP does neither require postsynaptic NMDAR nor L-type VGCC activation for induction. It rather depends on calcium release from postsynaptic internal stores mediated by $mGluR_{1,5}$-dependent activation of IP3 receptors in the ER (1.). This initial postsynaptic Ca^{2+} rise is amplified by Ca^{2+} dependent Ca^{2+} release via Ryanodine receptors (RyRs; 2.). Moreover, the 6 x 1:4 t-LTP depends (like 6 x 1:1 t-LTP) on the activation of cp-AMPARs. Intact D2 receptor signaling is mandatory to observe 6 x 1:4 t-LTP and might be involved in recruiting cp-AMPARs to the postsynaptic membrane (3.) for sustained Ca^{2+} influx during ongoing low frequency synaptic stimulation after t-LTP induction (4.). The resulting prolonged postsynaptic Ca^{2+} elevation initiated by mGluRs, RyRs, and cp-AMPARs leads to postsynaptic expression of 6 x 1:4 t-LTP by insertion of new GluA1 and GluA2-containing AMPARs into the postsynaptic membrane (5.)*

487 The scheme presented in **figure 9** summarizes our findings for the presynaptically expressed 6 x 1:1 t-LTP
488 and the postsynaptically expressed 6 x 1:4 t-LTP and suggests the putative roles of mGluRs, cp-AMPARs,
489 dopamine signaling, and internal Ca^{2+} stores in low repeat t-LTP. However, since the distribution of
490 dopaminergic fibers and the pre- and/or postsynaptic dopamine receptor localization in the CA1 region
491 and is not yet completely clear (compare Edelmann and Lessmann, 2018), further experiments are clearly
492 required to improve the mechanistic understanding of this aspect of low repeat t-LTP. None withstanding,
493 both low repeat t-LTP forms are already by now clearly distinguishable. Their different features of
494 induction and expression mechanisms and the distinct signaling cascades they employ likely form the basis
495 for the versatile computing capacity of individual CA1 neurons in the hippocampus.
496
497

498 **Discussion**

499 Our study shows that t-LTP at hippocampal SC-CA1 synapses requires only six repeats of coincident
500 presynaptic stimulation paired with either 1 or 4 postsynaptic spikes at low frequency (0.5 Hz). For the 1:4
501 burst protocol, even just three repeats are sufficient to elicit t-LTP. The 6 x 1:1 t-LTP could be induced by
502 Ca^{2+} influx via postsynaptic NMDARs and L-type VGCCs, occurred independent of BDNF release, and
503 required combined D1/D2 receptor signaling. In contrast, the 6 x 1:4 t-LTP was induced by postsynaptic
504 Ca^{2+} release from internal stores mediated via mGluRs/IP_3 signaling and ryanodine receptors, and was
505 completely inhibited in the presence of D2 receptor antagonists. Both, low repeat canonical and burst t-
506 LTP, strongly depended on activation of GluA2-lacking cp-AMPARs. These data suggest that low repeat
507 STDP paradigms with potentially high physiological relevance can induce equally robust t-LTP as observed
508 for high repeat t-LTP in the hippocampus. However, the pharmacological profile of low repeat t-LTP
509 induction and expression revealed astonishingly subtle differences between both induction protocols.

510

511 **Dependence of t-LTP on repeat number and frequency of the STDP stimulation**

512 Both 6 x t-LTP protocols used in our study yielded robust t-LTP with similar time courses as described
513 previously for standard STDP paradigms that used either higher number of pairings or higher pairing
514 frequency (compare e.g., Carlisle et al., 2008; Couey et al., 2007; Edelmann et al., 2015; Seol et al., 2007;
515 Tigaret et al., 2016; Wittenberg and Wang, 2006; Yang and Dani, 2014). To date, only few studies focused
516 on STDP protocols with low numbers of repeats for t-LTP induction (Cui et al., 2016; discussed in Edelmann
517 et al., 2017; Froemke et al., 2006; Zhang et al., 2009). Since only such low repeat t-LTP protocols can be
518 completed within a few seconds, these protocols are likely to represent a very physiological model for
519 synaptic plasticity events triggering learning and memory processes that can also occur on a timescale of
520 seconds. Thus, investigating the underlying signaling mechanisms appears to be relevant for learning
521 induced synaptic changes *in vivo*. Similar to the results of Froemke and colleagues (Froemke et al., 2006)
522 for layer 2/3 cortical neurons, we observed no significant difference in the magnitude of 1:1 t-LTP between
523 the threshold repeat number (i.e., 6 repeats at 0.5 Hz) and higher repeat numbers at hippocampal Schaffer
524 collateral (SC)–CA1 synapses (25 and 70 repeats; compare **Fig 1A**). As for the canonical protocol, we also
525 determined the threshold for successful t-LTP induction also for the burst protocol (compare **Fig 1B**). The
526 observed shift of the threshold repeat number to lower values (3 instead of 6 repeats for successful 1:4 t-
527 LTP induction) for the burst protocol speaks in favor of facilitated postsynaptic induction by the spike train
528 instead of single spikes used by the 1:1 protocol (compare Remy and Spruston, 2007). Although 35 repeats
529 of the burst protocol showed a tendency towards reduced magnitude of t-LTP, the efficacy of 3, 6 and 35
530 repeats of 1:4 t-LTP were not significantly different. Together these data suggest that depending on the
531 exact pattern (e.g., 1:1 vs. 1:4 paradigm) used for t-LTP induction distinct thresholds for the successful
532 number of repeats can be observed.

533 Bittner and colleagues recently described in elegant *in vivo* recordings synaptic plasticity in mouse
534 hippocampal place cells that can be triggered by pairing low numbers of postsynaptic action potentials
535 with long-lasting dendritic depolarization, which works equally well with positive and negative pairing
536 delays of roughly 1 s (Bittner et al., 2015; Bittner et al., 2017). While their work provides compelling
537 evidence for the physiological relevance of low repeat spiking induced LTP for learning, this behavioral
538 time scale synaptic plasticity follows a non-hebbian mechanism. In contrast, our low repeat t-LTP follows
539 hebbian rules, since only simultaneous and nearly coincident pre- and postsynaptic pairing with positive
540 timing delays leads to associative potentiation (compare **Fig 2C**). Nevertheless, also such hebbian t-LTP
541 protocols have been described previously to allow extension of STDP to behavioral time scales (compare
542 e.g., Drew and Abbott, 2006; Gerstner et al., 2018; Shindou et al., 2019). In case of our low repeat t-LTP
543 protocols, with the six repeat protocol comprising overall 10 s, and the three repeat protocol occurring
544 within overall 6 s, this duration might bridge the time window between millisecond-dependent STDP and
545 learned behavior on the time scale of several seconds.

546

547 In cultured hippocampal neurons, Zhang and colleagues (Zhang et al., 2009) showed that more than 10
548 repeats of their 1:1 STDP protocol were necessary to induce t-LTP. However, bath application of dopamine
549 facilitated t-LTP induction and reduced the number of pairings that were required at a given frequency to
550 successfully induce t-LTP (Zhang et al., 2009). Since primary cultures of dissociated hippocampal neurons
551 develop synaptic connections in the absence of dopaminergic inputs, the role of endogenous DA can be
552 investigated only if t-LTP is recorded in acutely isolated hippocampal slices as performed here.
553 Interestingly, our data show that both low repeat t-LTP variants tested are blocked when signaling of
554 endogenously released DA is inhibited (**Fig 6**). Our results are in line with the previously described effects
555 of exogenously added DA on t-LTP in hippocampal cultures (Zhang et al., 2009). The release of endogenous
556 DA in our slices (Edelmann and Lessmann, 2011, 2013) is therefore likely to account for the low number
557 of repeats required for successful induction of t-LTP in our study. Whether this effect is due to acute
558 release of DA from axon terminals elicited via the extracellular co-stimulation of dopaminergic afferents
559 during t-LTP induction and test stimulation or rather depends on ambient levels of DA in the slices remains
560 to be determined.

561 Regarding the magnitude of t-LTP induced by low repeat canonical and burst protocols we, found that
562 both, 6 x 1:1 and 6 x 1:4 t-LTP, were equally successful to induce t-LTP at positive spike timings (**Fig 2C**).
563 Because it is reasonable to assume that 1:4 burst protocols induce longer lasting and stronger Ca^{2+}
564 elevations than 1:1 pairings, it might be expected that the time course of synaptic potentiation could differ
565 between the two protocols. However, both protocols induced t-LTP with comparable onsets and rise times
566 of potentiation and also resulted in similar magnitudes of t-LTP after 1 h of recording (compare **Fig 2D**).
567 Thus, except for the lower threshold number of repeats to elicit t-LTP (see last paragraph), the burst
568 protocol does not seem to be more effective in inducing t-LTP at SC-CA1 synapses than the canonical
569 protocol.

570 We also compared different spike timings (with negative and positive delays), to compare the full capacity
571 to induce bidirectional plasticity with low repeat protocols (**Fig 2A, B**). For positive pairings with Δt: +20
572 ms we observed a similar decline (compared to Δt: +10 ms) in t-LTP magnitude as described previously for
573 higher numbers of repeats (compare Bi and Poo, 1998; Edelmann et al., 2015). When applying negative
574 pairings (i.e. post before pre pairings) t-LTP was absent, but we did not observe robust t-LTD for either of
575 the two protocols. While these results stress that successful induction of t-LTP is critically dependent on
576 the sequence of presynaptic and postsynaptic spiking and on the pairing interval, future studies should
577 address under which conditions low repeat t-LTD can be induced by anti-causal synaptic activation.

578

579 **Mechanisms of expression of low repeat t-LTP**

580 Despite the similarities described above, both low repeat protocols recruited different expression
581 mechanisms. Synaptic potentiation induced with the 6 x 1:1 protocol is most likely expressed by
582 presynaptic alterations (see below), whereas the 6 x 1:4 protocol relies on postsynaptic insertion of AMPA
583 receptors (**Fig 3**). Commonly, LTP at SC-CA1 synapses that is induced by high-frequency stimulation and is
584 also thought to be expressed by a postsynaptic increase in AMPA receptor mediated currents (Granger
585 and Nicoll, 2014; Nicoll, 2003). For STDP, however, different mechanisms of expression have been
586 described that varied between brain regions and depending on experimental conditions (see e.g., Costa
587 et al., 2017). Even at a given type of synapse (i.e. hippocampal SC-CA1) t-LTP can be expressed either pre-
588 or postsynaptically (Edelmann et al., 2015). At this synapse, the expression mechanism of LTP seemed to
589 be encoded by the pairing pattern used for STDP. While t-LTP induced by 70 x 1:1 stimulation was
590 expressed via increased presynaptic glutamate release, a 35 x 1:4 t-LTP was expressed via insertion of
591 additional AMPARs by a GluA1-dependent mechanism (Edelmann et al., 2015). However, in this previous
592 study, we used different numbers of repeats for the two t-LTP protocols (i.e. 20-35 x 1:4 and 70-100 x 1:1)
593 to keep postsynaptic activity at an equivalent level. Those previous results did not allow to distinguish
594 whether repeat number or stimulation pattern determined the site of t-LTP expression. With help of our
595 current experiments using fixed numbers of repeats for both protocols, we could now determine that the

596 pattern of postsynaptic spiking and not the repeat number influences the expression locus for t-LTP
597 (compare **Fig 3**).
598
599 For the 6 x 1:1 t-LTP, the absence of an increase in AMPAR mediated currents (**Fig 5**) and the observed
600 decrease in paired pulse ratio (PPR) after successful LTP induction and the increased mEPSC frequency
601 (**Fig S1**), are consistent with presynaptic enhancement of glutamate release probability.
602 Regarding the retrograde messenger required for both types of 1:1 t-LTP our data indicate that neither
603 NO nor endocannabinoids are involved in the presynaptic expression (data not shown). However, further
604 investigating the underlying presynaptic mechanisms of 6 x 1:1 t-LTP was beyond the scope of the current
605 study. The six repeat version of our burst t-LTP protocol (6 x 1:4) seems to follow the suggested
606 mechanisms for conventional SC-CA1 LTP, with postsynaptic expression via insertion of new AMPARs
607 leading to increased increased AMPAR mediated currents and the absence of significant changes in paired
608 pulse facilitation, as previously also described for high repeat burst t-LTP (Edelmann et al., 2015).
609 Furthermore, our experiments with Pep1-TGL clearly demonstrate the importance of GluA1 containing
610 AMPARs for the expression of 6 x 1:4 t-LTP (**Fig 3C**).
611
612 **Dependence of low repeat t-LTP induction on different sources for postsynaptic Ca^{2+} elevation**
613
614 Induction of t-LTP with low repeat STDP protocols as a model to investigate physiologically relevant
615 synaptic plasticity mechanisms has just started. Accordingly, the contribution of different sources of Ca^{2+}
616 to its induction was until now largely unknown. Unexpectedly, our experiments revealed distinctly
617 different routes for postsynaptic Ca^{2+} elevation for the low repeat 1:1 and 1:4 protocol to induce t-LTP.
618 The results for the 6 x 1:1 t-LTP are in accordance with previous studies showing that t-LTP as well as
619 classical high frequency stimulation induced LTP at CA1 glutamatergic synapses rely on Ca^{2+} influx via
620 postsynaptic NMDA receptors (Malenka and Bear, 2004). For STDP, NMDARs are thought to serve as
621 coincidence detectors of timed pre- and postsynaptic activation (e.g., Bi and Poo, 1998; Debanne et al.,
622 1998; Edelmann et al., 2015; Feldman, 2000). Depending on the level of postsynaptic Ca^{2+} that is reached
623 during induction, separate signaling cascades leading to either LTP or LTD are activated (Artola and Singer,
624 1993; cited in Caporale and Dan, 2008; Lisman, 1989). For t-LTD, alternative mechanisms for coincidence
625 detection have been described (Bender et al., 2006; Fino and Venance, 2010). Instead of NMDAR-
626 mediated Ca^{2+} influx, these studies reported that either mGluRs, L-type VGCCs or IP3 gated internal Ca^{2+}
627 stores can trigger the induction of LTD. As for LTD, also for LTP, additional coincidence detectors and Ca^{2+}
628 sources might be involved in its induction (Dudman et al., 2007; VGCC: Magee and Johnston, 1997; Nanou
629 et al., 2016; IP3-sensitive stores: Takechi et al., 1998; Wang et al., 2016; Wiera et al., 2017). In accordance
630 with these previous studies, we found that 6 x 1:1 t-LTP can in addition to NMDARs also be induced by
631 Ca^{2+} entry through L-type VGCCs (**Fig 4A, C**).
632 In contrast to these conventional Ca^{2+} sources for the canonical low repeat t-LTP, the situation is much
633 different for 6 x 1:4 burst t-LTP. Although a requirement for postsynaptic Ca^{2+} elevation is clearly evident
634 from the BAPTA experiments (**Fig 5A**), Ca^{2+} entry via NMDARs or VGCCs was not involved (compare **Fig 4B,**
635 **D**). Rather, our results demonstrated that the initial postsynaptic Ca^{2+} rise required for this atypical form
636 of hebbian plasticity involved group I mGluRs (i.e. $mGluR_1$ and $mGluR_5$), subsequent activation of IP_3Rs
637 and RyRs, eventually activating GluA2-lacking Ca^{2+}-permeable AMPARs in the postsynaptic membrane
638 (compare **Figs 5** and **8**). While activation of mGluRs accounts for the initial postsynaptic Ca^{2+} rise in 6 x 1:4
639 t-LTP, subsequent Ca^{2+} induced Ca^{2+} release via RyRs amplifies and prolongs this Ca^{2+} signal (compare **Fig**
640 **5D**). The initial rise in postsynaptic Ca^{2+} levels is most likely mediated by either Ca^{2+} influx through GluA2
641 subunit deficient Ca^{2+}-permeable AMPA receptors (cp-AMPARs) into the postsynaptic cell (Suzuki et al.,
642 2001) or driven by activation of mGluRs (Kaar and Rae, 2015). This is evident from our experiments
643 performed in the presence of the mGluR antagonists, IP_3R inhibitors and the antagonists of Ca^{2+}

644 permeable AMPARs NASPM and IEM, which completely inhibited 6 x 1:4 t-LTP (group I mGluR: **Fig 5B**, C,
645 cp-AMPAR: **Fig 8B, D**, for discussion of cp-AMPAR, see below).

646 Group I metabotropic GluR have indeed been described previously to be contribute to certain types of
647 hippocampal LTP (Wang et al., 2016), while our present results show for the first time their involvement
648 in STDP. Altogether it seems plausible that 6 x 1:4 stimulation first activates $mGluR_{1,5}$ receptors, which
649 subsequently trigger IP_3- mediated calcium release from internal stores (Jong et al., 2014, compare **Fig**
650 **5D**). The resulting calcium rise and additional Ca^{2+} influx via cp-AMPARs might than be strengthened by
651 additional IP_3 and RyR mediated calcium induced Ca^{2+} release to successfully boost low repeat induced
652 burst t-LTP (compare **Fig 9**).

653

654 **Regulation of low repeat t-LTP by dopamine receptor signaling**

655

656 The accurate timing of pre- and postsynaptic activity is necessary for hebbian plasticity. In addition,
657 neuromodulator signaling critically regulates the efficacy of STDP protocols to elicit t-LTP (e.g., Cassenaer
658 and Laurent, 2012; Cui et al., 2015; Edelmann et al., 2015; Edelmann et al., 2017; Edelmann and Lessmann,
659 2011, 2018; Pawlak and Kerr, 2008; Seol et al., 2007; Yang and Dani, 2014; Zhang et al., 2009). Since high
660 repeat STDP in the hippocampus is regulated by dopamine (DA, e.g., Edelmann and Lessmann, 2013), we
661 also investigated DAergic modulation of our two low repeat STDP variants (compare **Fig 6**). While both
662 low repeat t-LTP protocols were dependent on endogenous DA signaling, the pharmacological profile for
663 them was quite different. The 6 x 1:4 t-LTP was completely dependent on intact D2 receptor signaling, but
664 independent from D1 receptor activation. This result can be easily reconciled with pure D2 receptor
665 dependent signaling being responsible for induction of the 6 x 1:4 t-LTP (compare **Fig 6B**). Little is known
666 about D2R mediated function in t-LTP as well as classical LTP. It was shown, however, that D2 receptors
667 can limit feedforward inhibition in the prefrontal cortex and allow thereby more effective t-LTP (Xu and
668 Yao, 2010). Importantly, D2 like receptors are expressed in the hippocampus in pre- and postsynaptic
669 neurons and have been described to regulate synaptic plasticity (Beaulieu and Gainetdinov, 2011;
670 Dubovyk and Manahan-Vaughan, 2019; Sokoloff et al., 2006). Moreover, D2 receptors contribute to
671 hippocampus-dependent cognitive functions (Nyberg et al., 2016). Together, these previous results on D2
672 receptor mediated functions in the hippocampus are clearly in line with the role in 6 x 1:4 t-LTP in our
673 experiments. In contrast to the 6 repeat burst protocol, the 6 x 1:1 t-LTP remained functional when either
674 D1-like or D2-like dopamine receptor signaling was intact. Although inhibition of D2 receptors by Sulpiride
675 had a tendency to reduce the magnitude of the 1:1 t-LTP, this effect did not reach statistical significance.
676 Moreover, while the D1 receptor inhibitor SCH23390 alone did not show any signs of 6 x 1:1 t-LTP
677 inhibition, it was nevertheless able to impair the slightly reduced t-LTP in the presence of Sulpiride down
678 to control levels, when both antagonists were co-applied (**Fig 6A**). The interpretation of this
679 pharmacological profile of 6 x 1:1 t-LTP needs to take into consideration that D1-like and D2-like receptors
680 do not signal exclusively via altering cAMP levels (cAMP increase via D1-like receptors - or decreased via
681 D2-like receptors; Tritsch and Sabatini, 2012). Rather, D5 receptors and heterodimeric D1/D2 receptors
682 can also activate cAMP-independent PLC pathways stimulating in turn IP_3/Ca^{2+}, DAG/PKC signaling, or
683 MAPK signaling downstream of D1 receptor activation and Akt kinase signaling. Also direct modulation of
684 NMDARs and VGCCs in response to D2R activation is possible (Beaulieu and Gainetdinov, 2011).
685 Consequently, the question whether the combined D1 -like/D2 -like receptor dependence of the 1:1 t-LTP
686 reflects rather the activation of D1/D2 heteromeric receptors, or distinct pre- vs. postsynaptic expression
687 and signaling of D1 and D2 receptors at SC-CA1 synapses needs to be addressed by future experiments.

688 To interpret the combined regulation of the 6 x 1:1 t-LTP by D1- and D2-like receptors it also needs to be
689 taken into consideration that D2-like receptors are generally believed to display a higher affinity for DA
690 compared to D1-like receptors (Beaulieu and Gainetdinov, 2011). Therefore, the complex D1- and D2
691 receptor-dependent regulation of 6 x 1:1 t-LTP might assure that this type of t-LTP is on the one hand
692 regulated by the presence of DA, but on the other hand remains intact at high and low DA concentrations.

693 On the same vein, this co-regulation could assure that slowly rising ambient DA levels created by tonic
694 firing of DAergic neurons are equally effective in regulating 6 x 1:1 t-LTP as much faster rising DA
695 concentrations during phasic firing.

696 Such a change in DA release was indeed shown in recordings of midbrain neurons, where activity of
697 DAergic neurons switches from tonic to phasic burst activity resulting in locally distinct levels of secreted
698 DA in the target regions (Rosen et al., 2015). Local DA concentration differences can then result in
699 different DA-dependent effects, with high affinity D2-like receptors being activated by low and slowly
700 rising extracellular DA levels, while low affinity D1 receptors are only activated by local DA peaks.

701 For our STDP experiments where DAergic input fibers are most likely co-activated during SC stimulation,
702 we observed similar activity-dependent recruitment of different DA receptors. While D1 receptor-
703 dependent effects were activated by 70-100 stimulations (Edelmann and Lessmann, 2011 and compare
704 **Fig 6C**), D1/D2 receptors or pure D2 receptor mediated processes were already activated by six
705 presynaptic co-stimulations of DAergic fibers (compare **Fig 6A, B**). Taking into account that D2-like
706 receptors (i.e. D2, D3 and D4 receptors) are classically thought to inhibit LTP by decreasing cAMP/PKA
707 signaling (Otmakhov and Lisman, 2002; Otmakhova et al., 2000), D2-like receptor driven t-LTP processes
708 might indeed be activated by $G_{\beta\gamma}$ signaling independent of cAMP pathways. As mentioned above, $G_{\beta\gamma}$
709 signaling also blocks L-type and N-type VGCCs (Tritsch and Sabatini, 2012) and D2 receptor signaling can
710 yield Ca^{2+} release from internal stores - two mechanisms that might account for the uncommon type of
711 calcium source required for the induction of our 6 x 1:4 t-LTP (compare **Figs 4 and 5**).

712

713 **Dependence of low repeat t-LTP on BDNF/TrkB signaling**

714

715 Brain-derived neurotrophic factor (BDNF) is well known for its important role in mediating long-lasting
716 changes of synaptic plasticity (reviewed in e.g., Edelmann et al., 2014; Gottmann et al., 2009; Lessmann
717 et al., 2003; Park and Poo, 2013). Moreover, BDNF is also involved in regulating STDP (Edelmann et al.,
718 2015; Lu et al., 2014; Sivakumaran et al., 2009). For hippocampal SC-CA1 synapses it was shown that BDNF
719 is secreted from postsynaptic CA1 neurons in response to 20-35 repeats of a 1:4 STDP protocol mediating
720 postsynaptically expressed t-LTP via postsynaptic TrkB receptor activation (Edelmann et al., 2015).
721 Interestingly, the results of the present study revealed, that neither of the two low repeat t-LTP variants
722 depended on BDNF induced TrkB signaling (compare **Fig 7**). This finding was not unexpected since release
723 of endogenous BDNF has been reported previously to require more prolonged barrages of AP firing than
724 just 6 repeats of short AP (burst) firing at 0.5 Hz (compare Balkowiec and Katz, 2002; Edelmann et al.,
725 2015; Lu et al., 2014). This BDNF independency was observed in situations with either chronic (e.g.,
726 heterozygous BDNF knockout animals) or acute depletion of BDNF (BDNF scavenger; see e.g., Edelmann
727 et al., 2015; Meis et al., 2012; Schildt et al., 2013).

728

729 **Function of GluA2-lacking Ca^{2+} permeable AMPA receptors in low repeat t-LTP**

730

731 Interestingly, both variants of low repeat t-LTP were strictly dependent on activation of GluA2-lacking
732 calcium-permeable (cp-)AMPA receptors (**Fig 8**). In the respective experiments, NASPM or IEM were
733 present in the ACSF from the start of the recording to assure complete inhibition of cp-AMPARs during t-
734 LTP induction. The respective solvent controls were treated in the same way. In CA1 neurons, cp-AMPARs
735 were described to be absent from postsynaptic membranes during basal synaptic stimulation. Rather,
736 they were reported to transiently insert into the postsynaptic membrane after tetanic LTP stimulation to
737 allow sustained Ca^{2+} influx into the postsynaptic neuron after LTP induction, thereby facilitating
738 expression of late LTP (reviewed in Park et al., 2018). A role of cp-AMPARs in STDP has thus far not been
739 reported and these results represent a crucial new finding that emerge from our study. Additional
740 experiments will be required to determine the time course of activity-dependent cp-AMPAR incorporation

741 during induction of low repeat t-LTP into the postsynaptic membrane. Furthermore, it needs to be
742 determined how cp-AMPAR mediated Ca^{2+} influx is orchestrated with mGluR- and RyR-dependent Ca^{2+}
743 elevation for induction of low repeat 6 x 1:4 t-LTP. Likewise, the co-operation of cp-AMPARs with NMDAR-
744 and VGCC-dependent Ca^{2+} elevations for inducing 6 x 1:1 t-LTP needs to be investigated.

745 In addition to allowing sufficient Ca^{2+} elevation in t-LTP, cp-AMPARs might be involved in DA-dependent
746 priming of synapses for delayed/retroactive reinforcement of LTP or silent eligibility traces (e.g., Brzosko
747 et al., 2015; Gerstner et al., 2018; He et al., 2015; Shindou et al., 2019). By those eligibility traces or
748 delayed reinforcements, the different time scales between milliseconds and seconds can be bridged, to
749 connect hebbian synaptic plasticity to behavioral responses and learning. Such mechanisms might also be
750 involved in the signaling mechanisms employed by our low repeat t-LTP protocols (6 x 1:1 and 6 x 1:4),
751 since both variants of t-LTP show a clear dependence on DA signaling and on cp-AMPARs (compare **Figs 6**
752 and **8**).

753

754 In summary, we used two different low repeat STDP protocols at SC-CA1 synapses to record synaptic
755 plasticity at the single cell level in postsynaptic CA1 neurons (i.e. t-LTP). We found that, dependent on
756 stimulation pattern and repeat number, distinct signaling and expression mechanisms are activated by
757 the canonical and the burst low repeat paradigm. From our experiments, we can conclude that even with
758 the same experimental setup, age and species, multiple types of synaptic plasticity mechanisms can
759 coexist at a given type of synapse. This plethora of coexisting plasticity mechanisms for strengthening
760 synaptic transmission seems to be ideally suited to empower the hippocampus to fulfill its multiplexed
761 functions in memory storage.

762

763

764 **Material and Methods**

765

766 **Preparation of hippocampal slices**

767 Horizontal hippocampal slices (350 µm thickness) were prepared from 4 weeks old male wild type
768 C57BL/6J (Charles River), $BDNF^{+/-}$ or littermate control mice (Korte et al., 1995; all animals bred on a
769 C57BL/6J background), according to the ethical guidelines for the use of animal in experiments, and were
770 carried out in accordance with the European Committee Council Directive (2010/63/EU) and approved by
771 the local animal care committee (Landesverwaltungsamt Sachsen-Anhalt).

772 Briefly, mice were decapitated under deep anesthesia with forene (Isofluran CP, cp-pharma, Germany)
773 and the brain was rapidly dissected and transferred into ice-cold artificial cerebrospinal fluid (ACSF)
774 cutting solution (125 mM NaCl, 2.5 mM KCl, 0.8 mM NaH_2PO_4, 25 mM $NaHCO_3$, 25 mM Glucose, 6 mM
775 $MgCl_2$, 1 mM $CaCl_2$; pH 7.4; 300-303 mOsmol/kg), saturated with 95% O_2 and 5% CO_2. Blocks from both
776 hemispheres containing the hippocampus and the entorhinal cortex were sectioned with a vibratome (VT
777 1200 S, Leica, Germany). Slices were incubated for 35 min at 32°C in a handmade interface chamber
778 containing carboxygenated ACSF cutting solution and then transferred to room temperature (~21°C) for
779 at least 1 hour before the recording started. Whole cell patch-clamp recordings were performed in
780 submerged slices in a recording chamber with continuous perfusion (1-2 ml per min) of pre-warmed (30
781 ± 0.2°C) carboxygenated physiological ACSF solution (125 mM NaCl, 2.5 mM KCl, 0.8 mM NaH_2PO_4, 25 mM
782 $NaHCO_3$, 25 mM Glucose, 1 mM $MgCl_2$, 2 mM $CaCl_2$; pH 7.4; 300-303 mOsmol/kg). For all experiments,
783 100 µM Picrotoxin ($GABA_A$ blocker) was added to ACSF solution. Epileptiform activity by activation of
784 recurrent CA3 synapses was prevented by a cut between CA3 and CA1 subfields (compare Edelmann et
785 al., 2015). To reduce the amount of inhibitors in some of the experiments (e.g. application of NASPM and
786 IEM-1460) we used a micro-perfusion pump-driven solution recycling system (Bioptechs Delta T Micro-
787 Perfusion pump high flow, ChromaPhor, Germany) to limit the volume of solution for incubation of slices
788 (Meis et al., 2012). Both, NASPM and IEM were applied 15 min prior to STDP induction. The drugs were

present during the whole experiment. Respective matched control experiments were performed under identical conditions to assure that the microperfusion recycling of ACSF alone did not affect t-LTP.

Electrophysiological recordings

Whole cell patch-clamp recordings were performed on pyramidal neurons in the CA1 subregion of the intermediate hippocampus under visual control with infrared DIC-videomicroscopy (RT-SE series; Diagnostic instruments, Michigan, USA). The pipettes (resistance 5-7 MΩ) were filled with internal solution containing (in mM): 10 HEPES, 20 KCl, 115 potassium gluconate, 0-0.00075 $CaCl_2$, 10 Na phosphocreatine, 0.3 Na-GTP, and 4 Mg-ATP (pH 7.4, 285-290 mOsmol/kg). Cells were held at -70 mV in current clamp or voltage clamp (liquid junction potential of +10 mV of internal solution was corrected manually) with an EPC-8 patch clamp amplifier (HEKA, Lamprecht, Germany). Extracellular stimulation of the Schaffer collateral (SC) fibers to generate an excitatory postsynaptic potential (EPSP, at 0.05Hz) was induced either by glass stimulation electrodes (resistance 0.7 – 0.9 MΩ) or a concentric bipolar electrode (FHC; Bowdoin, USA) positioned in Stratum radiatum (SR) of the CA1 subregion. The stimulus intensity was adjusted to evoke responses with amplitudes of 4-5 mV corresponding to 30-50% of maximal EPSP amplitudes. Stimulus duration was set to 0.7 ms with intensities ranging between 90 to 700 µA.

Induction of Spike timing-dependent plasticity

Spike timing-dependent plasticity (STDP) was induced by pairing of an individual EPSP, generated by extracellular stimulation of SC, with a single action potential (AP) or with a burst of 4 APs (frequency 200 Hz) induced by somatic current injection (2 ms; 1 nA) through the recording electrode (Edelmann et al., 2015). Pairings of postsynaptic EPSP and APs were usually performed with a time interval of +10 ms, and were repeated 2-70 times at a frequency of 0.5 Hz to elicit t-LTP. In some experiments, either longer time windows (positive spike timings: Δt= +17-25 ms, binned as 20 ms data) were used to test t-LTP at longer Δt or short negative spike timings (Δt= -15ms) were used to test effects of anti-causal synaptic stimulation. EPSPs were monitored every 20 s (i.e., 0.05 Hz) for 10 min baseline and then 30 min or 60 min after STDP induction. Unpaired stimulation of 4 postsynaptic APs instead of a full STDP protocol were performed (i.e., 6x 0:4) in a subset of cells that served as controls. In another set of cells, we assessed possible spontaneous changes in synaptic transmission (stimulation at 0.05 Hz for 40 min) in the absence of any STDP stimulation. These recordings served as negative controls (designated 0:0 controls).

To investigate whether a rise of postsynaptic Ca^{2+} concentration is required for induction of t-LTP under our conditions, we applied the Ca^{2+} chelator BAPTA (10 mM, Sigma, Germany) via the patch pipette solution into the recorded postsynaptic neuron. NMDA receptor (R) dependency was tested by application of an NMDAR antagonist (APV 50 µM, DL-2-Amino-5-phosphonopentanoic acid, Tocris, Germany) in the bath solution. The contribution of L-type voltage gated Ca^{2+} channel activation to t-LTP was evaluated with bath applied Nifedipine (25 µM, Sigma, Germany). To interfere with group I metabotropic glutamate receptor (mGluR) signaling we used bath application of either the $mGlu_1$ receptor antagonist YM298198 (1 µM, Tocris, Germany) or the $mGluR_5$ receptor antagonist MPEP (10 µM, Tocris, Germany) alone, or both blocker simultaneously (the substances were bath applied for a minimum of 15 min prior and during STDP recordings). IP3 receptors were blocked by bath application of 2-APB (100 µM, Tocris, Germany, micro-perfusion pump), 2-APB was applied at least 15 min prior t-LTP induction and was present throughout the recordings. Intracellular infusion of ryanodine (100 µM, Tocris, Germany, infusion for 15 min) was used to block ryanodine receptors of internal calcium stores. Where appropriate, respective controls were performed with ACSF or internal solution containing the same final concentration of DMSO as used for the drug containing solution (i.e. solvent controls) using the same perfusion conditions.

We investigated dopaminergic neuromodulation of STDP by bath application of specific antagonists for D1-like (SCH23390, SCH; 10 µM, Sigma) and D2-like dopamine receptors (Sulpiride, Sulp; 10 µM, Sigma, substances were applied for at least 15 min prior STDP recordings). The contribution of BDNF/TrkB

838 signaling was tested by bath application a scavenger of endogenous BDNF (recombinant human TrkB Fc
839 chimera, R&D Systems, Germany). For scavenging of BDNF, slices were pre-incubated for at least 3h with
840 5µg/ml TrkB-Fc, and subsequent recordings were performed in the presence of 100 ng/ml TrkB-Fc
841 (compare Edelmann et al., 2015). Positive controls were recorded in slices kept under the same regime,
842 but without the addition of TrkB-Fc. To test low repeat t-LTP under conditions of chronic 50% BDNF
843 reduction, we used heterozygous BDNF $^{+/-}$ mice and respective wildtype littermates as described
844 previously (Edelmann et al., 2015).

845 The contribution of activity-dependent incorporation of GluA1 subunit containing AMPA receptors to
846 expression of low repeat t-LTP was verified by postsynaptic application of Pep1-TGL (100 µM, Tocris,
847 Germany) via the patch pipette solution. To investigate a possible role of GluA2 lacking calcium permeable
848 (cp-) AMPA receptors, we use bath applied NASPM (1-Naphtyl acetyl spermine trihydrochloride, 100 µM,
849 Tocris, Germany) or IEM-1460 (*N*,*N*,*H*,-Trimethyl-5-[(tricyclo[3.3.1.13,7]dec-1-ylmethyl)amino]-1-
850 pentanaminiumbromide hydrobromide, 100 µM, Tocris, Germany).

851

852 **Data acquisition and Data Analysis**

853 Data were filtered at 3 kHz using a patch clamp amplifier (EPC-8, HEKA, Germany) connected to a LiH8+8
854 interface and digitized at 10 kHz using PATCHMASTER software (HEKA, Germany). Data analysis was
855 performed with Fitmaster software (HEKA, Germany). All experiments were performed in the current
856 clamp mode, except for paired pulse ratio (PPR) that was recorded in the voltage clamp mode at -70 mV
857 holding potential, and AMPA/NMDA receptor current ratios that were recorded in voltage clamp at -70
858 mV and -20 mV holding potential. The holding potential for recording of NMDAR currents was set to the
859 maximal depolarized value (i.e. -20mV) that allow stable recordings in spite of activated voltage gated K^+
860 currents. We did not replace K^+ for Cs^+ in our internal solutions, since we wanted to elicit LTP under
861 physiological conditions and AMPAR/NMDAR current ratio had to be measured before and 30 min after
862 t-LTP induction. Input resistance was monitored by hyperpolarizing current steps (250 ms; 20 pA), elicited
863 prior to evoked EPSP responses. The average slope calculated from 10 min control recording (baseline)
864 were set to 100% and all subsequent EPSP slopes of a cell were expressed as percentage of baseline
865 slopes. Synaptic strength was calculated from the mean EPSP slopes 20-30 min (or 50-60 min) after STDP
866 induction, divided by the mean EPSP slope measured during 10 min before STDP stimulation (baseline).
867 Spike timing intervals (i.e. *Δt,* ms) were measured as the time between onset of the evoked EPSP and the
868 peak of the first action potential. Cells were only included for analysis if the initial resting membrane
869 potential (RMP) was between -55 and -70 mV. Cells were excluded when the input resistance varied more
870 than 25% over the entire experiment. Furthermore, traces showing visible "run-up" or "run-down" during
871 baseline recording were excluded. Data were binned at 1 min intervals.

872 AMPA/NMDA receptor mediated current ratios were calculated from the peak current amplitudes of the
873 fast AMPA receptor mediated components evoked at a holding potential of -70 mV divided by the
874 amplitudes of the NMDAR mediated slow current components measured after 50 ms of the onset of the
875 EPSCs at a holding potential of -20 mV. Selectivity of this procedure for AMPAR and NMDAR mediated
876 currents was confirmed by bath application of either 50 µM APV or 10 µM NBQX in selected experiments
877 (compare Edelmann et al., 2015).

878 For analysis of presynaptic short-term plasticity before and after t-LTP induction, paired pulse facilitation
879 was recorded in voltage clamp mode at a holding potential of -70 mV, and the paired pulse ratio (PPR)
880 was determined by dividing the peak current amplitudes of the second EPSC by the first EPSC at an inter-
881 stimulus interval of 50 ms.

882 To further check for a presynaptic LTP expression locus of the 6x 1:1 t-LTP, coefficient of variance (CV)
883 analysis was performed. CV is expressed as standard deviation/mean (Faber and Korn, 1991). The ratio of
884 CV^2 before and after the pairing (20-30 min after induction) was plotted against the respective ratio of
885 mean EPSP slopes (EPSP after/EPSP baseline, Malinow and Tsien, 1990; Manabe et al., 1993). CV^2 ratio
886 was calculated by dividing $1/CV^2$ after LTP with $1/CV^2$ of baseline. Presynaptic LTP is supposed to influence

887 CV^2 more strongly than the EPSP amplitude so that values lie on or above the diagonal line of unity (Bender
888 et al., 2009; compare Edelmann et al., 2015). As an additional measure for possible t-LTP induced
889 presynaptic changes, putative miniature synaptic currents ("miniature" EPSCs; cut-off amplitude: 15pA to
890 minimize analyses of evoked responses) were analyzed with the Minianalysis program (Synaptosoft, USA)
891 from 3 min of continuous recordings before and 30 min after t-LTP induction. Cumulative fraction plots
892 for amplitudes and inter-event intervals (IEI) were generated. TTX was omitted when recording mEPSCs
893 to allow STDP induction under physiological conditions.

894 To verify independent expression of the two low repeat paradigms, we performed an occlusion approach.
895 Here we subsequently induced first 6 x 1:1 t-LTP and 25 min later the 6 x 1:4 t-LTP in the same cell and
896 compared the change in synaptic strength by the two protocols.

897 To assure reproducibility of results, data for experiments shown in **Figs 1, 3, 5, 8** and **S1** were pooled from
898 2 or 3 independent experimenters, blind to the results of the other(s).

899

900 **Statistics**

901 Statistical analysis was performed using GraphPad Prism version 6.0 (GraphPad Software, USA) or JMP 8
902 (SAS Institute Inc., USA). Pooled data of experiments from at least three different animals are expressed
903 as mean ± SEM. Paired and unpaired two tailed t-tests were used for data with normal distribution.
904 Otherwise nonparametric Mann-Whitney U-test was applied. Multiple comparisons were assessed with a
905 one-way analysis of variance (ANOVA), followed by a post hoc t-test Dunnet's test, or Kruskal-Wallis test,
906 followed by post hoc Dunn's test for parametric and nonparametric data. A p-value <0.05 was set as level
907 of significance and is indicated by an asterisk. The actual statistic procedures used for each experiment
908 are mentioned in the text. The respective number of experiments (n) and the number of animals (N) is
909 reported in the figure legends.

910

911 **Acknowledgments:**

912 The project was funded by the federal state of Saxony-Anhalt and the "European Regional Developmental
913 Fund (ERDF 2014-2020), Project: Center for Behavioral Brain Sciences (CBBS) FKS: ZS/2016/04/78113; by
914 the federal state Saxony-Anhalt and the European Structural and Investment Funds (ESF, 2014-2020),
915 project number ZS/2016/08/80645 and by the DFG ED 280/1-1 and SFB779/B06. The authors thank Regina
916 Ziegler for excellent technical assistance.

917

918 CRediT

919 Conceptualization: VL, EE; Methodology: VL, EE and EC-P; Investigation: EC-P, BK, GQ, SB with help by EE;
920 Writing: EE, VL, with help by EC-P; Funding Acquisition: VL, EE; Resources: VL; Supervision: VL, EE.

921

922 The authors declare no competing interests.

923

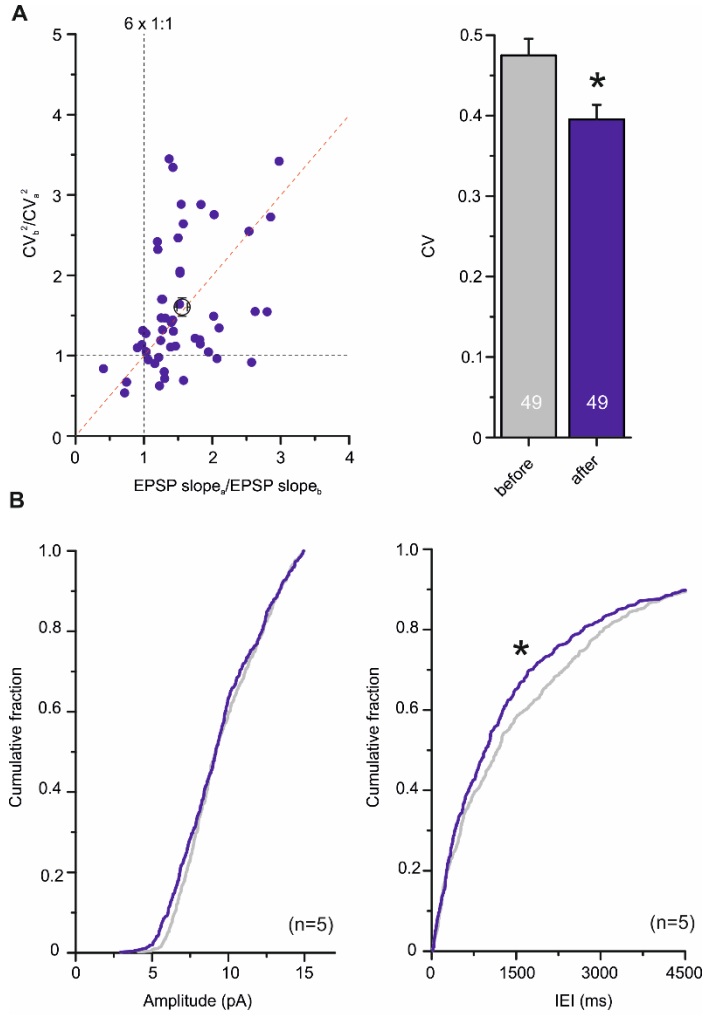

Figure S1: Evidence for presynaptic expression locus of 6 x 1:1 t-LTP. A*) CV² analysis. Left: Each point represents an individual cell subjected to 6 x 1:1 t-LTP stimulation. X-axis: magnitude of potentiation; y-axis: change in coefficient of variation. All points on or above the diagonal red line indicate presynaptic expression of 6x 1:1 t-LTP in the respective cell. Right: the average over all cells revealed a significant decrease of CV after t-LTP induction, being consistent with a presynaptic change.* ***B****) Cumulative fraction of mEPSC amplitudes (left) and interevent intervals (IEI; right) before and after 6 x 1:1 t-LTP induction. Blue color indicates cumulative probability after t-LTP induction (grey line: before t-LTP induction). The decrease in IEI (reflecting increased mEPSC frequencies) in the absence of change in mEPSC amplitudes (left) is consistent with a presynaptic change. Data are expressed as mean ± SEM. The analysis shows the results from 49 cells (in A) and 5 cells (B) from at least 3 different animals.*

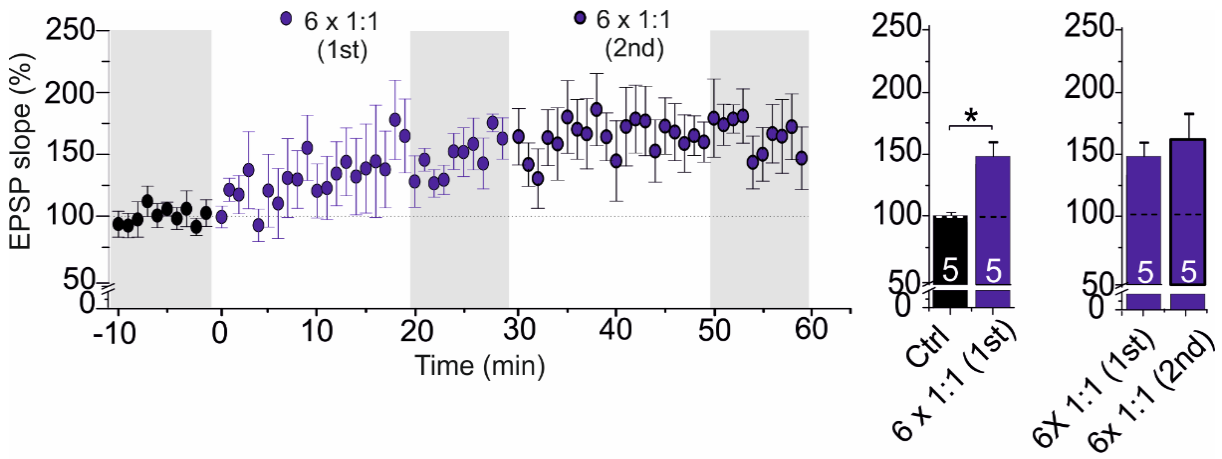

Figure S2: Two subsequent stimulations with the 6 x 1:1 t-LTP protocol do not yield additional potentiation. *SC-CA1 synapses were recorded as in* ***figure 8****, and 6 x 1:1 t-LTP stimulation was performed at 0 and 30 min in the same cells (n=5 / N= 3). The second induction protocol did not significantly increase the magnitude of t-LTP that was reached after the first t-LTP induction. Note that subsequent stimulations with the 6x 1:1 protocol followed by the 6 x 1:4 protocol in the same cells yielded additional and independent potentiation (compare* ***Fig 8****). Average time course of potentiation and mean (± SEM) magnitude of t-LTP are shown for the respective experiments.*

949 **References**

950 Artola, A., and Singer, W. (1993). Long-term depression of excitatory synaptic transmission and its
951 relationship to long-term potentiation. Trends Neurosci 16, 480-487.

952 Balkowiec, A., and Katz, D.M. (2002). Cellular mechanisms regulating activity-dependent release of native
953 brain-derived neurotrophic factor from hippocampal neurons. J Neurosci 22, 10399-10407.

954 Balschun, D., Manahan-Vaughan, D., Wagner, T., Behnisch, T., Reymann, K.G., and Wetzel, W. (1999). A
955 specific role for group I mGluRs in hippocampal LTP and hippocampus-dependent spatial learning. Learn
956 Memory 6, 138-152.

957 Banerjee, A., Meredith, R.M., Rodriguez-Moreno, A., Mierau, S.B., Auberson, Y.P., and Paulsen, O. (2009).
958 Double dissociation of spike timing-dependent potentiation and depression by subunit-preferring NMDA
959 receptor antagonists in mouse barrel cortex. Cereb Cortex 19, 2959-2969.

960 Beaulieu, J.M., and Gainetdinov, R.R. (2011). The physiology, signaling, and pharmacology of dopamine
961 receptors. Pharmacol Rev 63, 182-217.

962 Bender, V.A., Bender, K.J., Brasier, D.J., and Feldman, D.E. (2006). Two coincidence detectors for spike
963 timing-dependent plasticity in somatosensory cortex. J Neurosci 26, 4166-4177.

964 Bender, V.A., Pugh, J.R., and Jahr, C.E. (2009). Presynaptically expressed long-term potentiation increases
965 multivesicular release at parallel fiber synapses. J Neurosci 29, 10974-10978.

966 Bi, G.Q., and Poo, M.M. (1998). Synaptic modifications in cultured hippocampal neurons: dependence on
967 spike timing, synaptic strength, and postsynaptic cell type. J Neurosci 18, 10464-10472.

968 Bi, G.Q., and Poo, M.M. (2001). Synaptic modification by correlated activity: Hebb's postulate revisited.
969 Annu Rev Neurosci 24, 139-166.

970 Bittner, K.C., Grienberger, C., Vaidya, S.P., Milstein, A.D., Macklin, J.J., Suh, J., Tonegawa, S., and Magee,
971 J.C. (2015). Conjunctive input processing drives feature selectivity in hippocampal CA1 neurons. Nat
972 Neurosci 18, 1133-1142.

973 Bittner, K.C., Milstein, A.D., Grienberger, C., Romani, S., and Magee, J.C. (2017). Behavioral time scale
974 synaptic plasticity underlies CA1 place fields. Science 357, 1033-1036.

975 Bliss, T.V., and Cooke, S.F. (2011). Long-term potentiation and long-term depression: a clinical perspective.
976 Clinics (Sao Paulo) 66 Suppl 1, 3-17.

977 Bliss, T.V., and Lomo, T. (1973). Long-lasting potentiation of synaptic transmission in the dentate area of
978 the anaesthetized rabbit following stimulation of the perforant path. J Physiol 232, 331-356.

979 Brzosko, Z., Schultz, W., and Paulsen, O. (2015). Retroactive modulation of spike timing-dependent
980 plasticity by dopamine. Elife 4.

981 Buchanan, K.A., and Mellor, J.R. (2007). The development of synaptic plasticity induction rules and the
982 requirement for postsynaptic spikes in rat hippocampal CA1 pyramidal neurones. J Physiol 585, 429-445.

983 Caporale, N., and Dan, Y. (2008). Spike timing-dependent plasticity: a Hebbian learning rule. Annu Rev
984 Neurosci 31, 25-46.

985 Carlisle, H.J., Fink, A.E., Grant, S.G., and O'Dell, T.J. (2008). Opposing effects of PSD-93 and PSD-95 on long-
986 term potentiation and spike timing-dependent plasticity. J Physiol 586, 5885-5900.

987 Cassenaer, S., and Laurent, G. (2012). Conditional modulation of spike-timing-dependent plasticity for
988 olfactory learning. Nature 482, 47-52.

989 Chater, T.E., and Goda, Y. (2014). The role of AMPA receptors in postsynaptic mechanisms of synaptic
990 plasticity. Front Cell Neurosci 8, 401.

991 Costa, R.P., Mizusaki, B.E., Sjostrom, P.J., and van Rossum, M.C. (2017). Functional consequences of pre-
992 and postsynaptic expression of synaptic plasticity. Philos Trans R Soc Lond B Biol Sci 372.

993 Couey, J.J., Meredith, R.M., Spijker, S., Poorthuis, R.B., Smit, A.B., Brussaard, A.B., and Mansvelder, H.D.
994 (2007). Distributed network actions by nicotine increase the threshold for spike-timing-dependent
995 plasticity in prefrontal cortex. Neuron 54, 73-87.

996 Cui, Y., Paille, V., Xu, H., Genet, S., Delord, B., Fino, E., Berry, H., and Venance, L. (2015). Endocannabinoids
997 mediate bidirectional striatal spike-timing dependent plasticity. J Physiol.

998 Cui, Y., Prokin, I., Xu, H., Delord, B., Genet, S., Venance, L., and Berry, H. (2016). Endocannabinoid dynamics
999 gate spike-timing dependent depression and potentiation. Elife 5, e13185.
1000 Debanne, D., Gahwiler, B.H., and Thompson, S.M. (1998). Long-term synaptic plasticity between pairs of
1001 individual CA3 pyramidal cells in rat hippocampal slice cultures. J Physiol 507 (Pt 1), 237-247.
1002 Drew, P.J., and Abbott, L.F. (2006). Extending the effects of spike-timing-dependent plasticity to
1003 behavioral timescales. Proc Natl Acad Sci U S A 103, 8876-8881.
1004 Dubovyk, V., and Manahan-Vaughan, D. (2018). Less means more: The magnitude of synaptic plasticity
1005 along the hippocampal dorso-ventral axis is inversely related to the expression levels of plasticity-related
1006 neurotransmitter receptors. Hippocampus 28, 136-150.
1007 Dubovyk, V., and Manahan-Vaughan, D. (2019). Gradient of Expression of Dopamine D2 Receptors Along
1008 the Dorso-Ventral Axis of the Hippocampus. Front Synaptic Neurosci 11, 28.
1009 Dudman, J.T., Tsay, D., and Siegelbaum, S.A. (2007). A role for synaptic inputs at distal dendrites:
1010 instructive signals for hippocampal long-term plasticity. Neuron 56, 866-879.
1011 Edelmann, E., Cepeda-Prado, E., Franck, M., Lichtenecker, P., Brigadski, T., and Lessmann, V. (2015). Theta
1012 Burst Firing Recruits BDNF Release and Signaling in Postsynaptic CA1 Neurons in Spike-Timing-Dependent
1013 LTP. Neuron 86, 1041-1054.
1014 Edelmann, E., Cepeda-Prado, E., and Lessmann, V. (2017). Coexistence of Multiple Types of Synaptic
1015 Plasticity in Individual Hippocampal CA1 Pyramidal Neurons. Front Synaptic Neurosci 9, 7.
1016 Edelmann, E., and Lessmann, V. (2011). Dopamine Modulates Spike Timing-Dependent Plasticity and
1017 Action Potential Properties in CA1 Pyramidal Neurons of Acute Rat Hippocampal Slices. Front Synaptic
1018 Neurosci 3, 6.
1019 Edelmann, E., and Lessmann, V. (2013). Dopamine regulates intrinsic excitability thereby gating successful
1020 induction of spike timing-dependent plasticity in CA1 of the hippocampus. Front Neurosci 7, 25.
1021 Edelmann, E., and Lessmann, V. (2018). Dopaminergic innervation and modulation of hippocampal
1022 networks. Cell Tissue Res 373, 711-727.
1023 Edelmann, E., Lessmann, V., and Brigadski, T. (2014). Pre- and postsynaptic twists in BDNF secretion and
1024 action in synaptic plasticity. Neuropharmacology 76 Pt C, 610-627.
1025 Endres, T., and Lessmann, V. (2012). Age-dependent deficits in fear learning in heterozygous BDNF knock-
1026 out mice. Learn Mem 19, 561-570.
1027 Faber, D.S., and Korn, H. (1991). Applicability of the coefficient of variation method for analyzing synaptic
1028 plasticity. Biophys J 60, 1288-1294.
1029 Feldman, D.E. (2000). Timing-based LTP and LTD at vertical inputs to layer II/III pyramidal cells in rat barrel
1030 cortex. Neuron 27, 45-56.
1031 Feldman, D.E. (2012). The spike-timing dependence of plasticity. Neuron 75, 556-571.
1032 Fino, E., and Venance, L. (2010). Spike-timing dependent plasticity in the striatum. Front Synaptic Neurosci
1033 2, 6.
1034 Froemke, R.C., Tsay, I.A., Raad, M., Long, J.D., and Dan, Y. (2006). Contribution of individual spikes in burst-
1035 induced long-term synaptic modification. J Neurophysiol 95, 1620-1629.
1036 Gao, J., Voss, A.A., Pessah, I.N., Lauer, F.T., Penning, T.M., and Burchiel, S.W. (2005). Ryanodine receptor-
1037 mediated rapid increase in intracellular calcium induced by 7,8-benzo(a)pyrene quinone in human and
1038 murine leukocytes. Toxicol Sci 87, 419-426.
1039 Gerstner, W., Lehmann, M., Liakoni, V., Corneil, D., and Brea, J. (2018). Eligibility Traces and Plasticity on
1040 Behavioral Time Scales: Experimental Support of NeoHebbian Three-Factor Learning Rules. Front Neural
1041 Circuits 12, 53.
1042 Gottmann, K., Mittmann, T., and Lessmann, V. (2009). BDNF signaling in the formation, maturation and
1043 plasticity of glutamatergic and GABAergic synapses. Exp Brain Res 199, 203-234.
1044 Granger, A.J., and Nicoll, R.A. (2014). Expression mechanisms underlying long-term potentiation: a
1045 postsynaptic view, 10 years on. Philos T R Soc B 369.

1046 Hagena, H., and Manahan-Vaughan, D. (2016). Dopamine D1/D5, But not D2/D3, Receptor Dependency
1047 of Synaptic Plasticity at Hippocampal Mossy Fiber Synapses that Is Enabled by Patterned Afferent
1048 Stimulation, or Spatial Learning. Front Synaptic Neurosci 8, 31.
1049 Hayashi, Y., Shi, S.H., Esteban, J.A., Piccini, A., Poncer, J.C., and Malinow, R. (2000). Driving AMPA receptors
1050 into synapses by LTP and CaMKII: requirement for GluR1 and PDZ domain interaction. Science 287, 2262-
1051 2267.
1052 He, K., Huertas, M., Hong, S.Z., Tie, X., Hell, J.W., Shouval, H., and Kirkwood, A. (2015). Distinct Eligibility
1053 Traces for LTP and LTD in Cortical Synapses. Neuron 88, 528-538.
1054 Herring, B.E., and Nicoll, R.A. (2016). Long-Term Potentiation: From CaMKII to AMPA Receptor Trafficking.
1055 Annu Rev Physiol 78, 351-365.
1056 Jong, Y.J., Sergin, I., Purgert, C.A., and O'Malley, K.L. (2014). Location-dependent signaling of the group 1
1057 metabotropic glutamate receptor mGlu5. Mol Pharmacol 86, 774-785.
1058 Kaar, A., and Rae, M.G. (2015). Metabotropic glutamate receptor-mediated cyclic ADP ribose signalling.
1059 Biochem Soc Trans 43, 405-409.
1060 Kauer, J.A., and Malenka, R.C. (2006). LTP: AMPA receptors trading places. Nat Neurosci 9, 593-594.
1061 Korte, M., Carroll, P., Wolf, E., Brem, G., Thoenen, H., and Bonhoeffer, T. (1995). Hippocampal long-term
1062 potentiation is impaired in mice lacking brain-derived neurotrophic factor. Proc Natl Acad Sci U S A 92,
1063 8856-8860.
1064 Lalanne, T., Oyrer, J., Farrant, M., and Sjostrom, P.J. (2018). Synapse Type-Dependent Expression of
1065 Calcium-Permeable AMPA Receptors. Front Synaptic Neurosci 10, 34.
1066 Lee, H.K., and Kirkwood, A. (2011). AMPA receptor regulation during synaptic plasticity in hippocampus
1067 and neocortex. Semin Cell Dev Biol 22, 514-520.
1068 Lessmann, V., Gottmann, K., and Malcangio, M. (2003). Neurotrophin secretion: current facts and future
1069 prospects. Prog Neurobiol 69, 341-374.
1070 Lisman, J. (1989). A mechanism for the Hebb and the anti-Hebb processes underlying learning and
1071 memory. Proc Natl Acad Sci U S A 86, 9574-9578.
1072 Liu, Y., Cui, L., Schwarz, M.K., Dong, Y., and Schluter, O.M. (2017). Adrenergic Gate Release for Spike
1073 Timing-Dependent Synaptic Potentiation. Neuron 93, 394-408.
1074 Lu, H., Park, H., and Poo, M.M. (2014). Spike-timing-dependent BDNF secretion and synaptic plasticity.
1075 Philos Trans R Soc Lond B Biol Sci 369, 20130132.
1076 Lynch, M.A. (2004). Long-term potentiation and memory. Physiol Rev 84, 87-136.
1077 Magee, J.C., and Johnston, D. (1997). A synaptically controlled, associative signal for Hebbian plasticity in
1078 hippocampal neurons. Science 275, 209-213.
1079 Malenka, R.C., and Bear, M.F. (2004). LTP and LTD: an embarrassment of riches. Neuron 44, 5-21.
1080 Malinow, R., and Tsien, R.W. (1990). Presynaptic enhancement shown by whole-cell recordings of long-
1081 term potentiation in hippocampal slices. Nature 346, 177-180.
1082 Man, H.Y. (2011). GluA2-lacking, calcium-permeable AMPA receptors--inducers of plasticity? Curr Opin
1083 Neurobiol 21, 291-298.
1084 Manabe, T., Wyllie, D.J., Perkel, D.J., and Nicoll, R.A. (1993). Modulation of synaptic transmission and long-
1085 term potentiation: effects on paired pulse facilitation and EPSC variance in the CA1 region of the
1086 hippocampus. J Neurophysiol 70, 1451-1459.
1087 Markram, H., Gerstner, W., and Sjostrom, P.J. (2011). A history of spike-timing-dependent plasticity. Front
1088 Synaptic Neurosci 3, 4.
1089 Meis, S., Endres, T., and Lessmann, V. (2012). Postsynaptic BDNF signalling regulates long-term
1090 potentiation at thalamo-amygdala afferents. J Physiol 590, 193-208.
1091 Meredith, R.M., Floyer-Lea, A.M., and Paulsen, O. (2003). Maturation of long-term potentiation induction
1092 rules in rodent hippocampus: role of GABAergic inhibition. J Neurosci 23, 11142-11146.
1093 Missale, C., Nash, S.R., Robinson, S.W., Jaber, M., and Caron, M.G. (1998). Dopamine receptors: from
1094 structure to function. Physiol Rev 78, 189-225.

1095 Morita, D., Rah, J.C., and Isaac, J.T. (2014). Incorporation of inwardly rectifying AMPA receptors at silent
1096 synapses during hippocampal long-term potentiation. Philos Trans R Soc Lond B Biol Sci 369, 20130156.
1097 Mu, Y., and Poo, M.M. (2006). Spike timing-dependent LTP/LTD mediates visual experience-dependent
1098 plasticity in a developing retinotectal system. Neuron 50, 115-125.
1099 Nanou, E., Scheuer, T., and Catterall, W.A. (2016). Calcium sensor regulation of the CaV2.1 Ca2+ channel
1100 contributes to long-term potentiation and spatial learning. Proc Natl Acad Sci U S A 113, 13209-13214.
1101 Nevian, T., and Sakmann, B. (2006). Spine Ca2+ signaling in spike-timing-dependent plasticity. J Neurosci
1102 26, 11001-11013.
1103 Neyman, S., and Manahan-Vaughan, D. (2008). Metabotropic glutamate receptor 1 (mGluR1) and 5
1104 (mGluR5) regulate late phases of LTP and LTD in the hippocampal CA1 region in vitro. Eur J Neurosci 27,
1105 1345-1352.
1106 Nicoll, R.A. (2003). Expression mechanisms underlying long-term potentiation: a postsynaptic view. Philos
1107 T R Soc B 358, 721-726.
1108 Nicoll, R.A., and Malenka, R.C. (1995). Contrasting properties of two forms of long-term potentiation in
1109 the hippocampus. Nature 377, 115-118.
1110 Nyberg, L., Karalija, N., Salami, A., Andersson, M., Wahlin, A., Kaboovand, N., Kohncke, Y., Axelsson, J.,
1111 Rieckmann, A., Papenberg, G.*, et al.* (2016). Dopamine D2 receptor availability is linked to hippocampal-
1112 caudate functional connectivity and episodic memory. Proc Natl Acad Sci U S A 113, 7918-7923.
1113 Otmakhov, N., and Lisman, J.E. (2002). Postsynaptic application of a cAMP analogue reverses long-term
1114 potentiation in hippocampal CA1 pyramidal neurons. J Neurophysiol 87, 3018-3032.
1115 Otmakhova, N.A., Otmakhov, N., Mortenson, L.H., and Lisman, J.E. (2000). Inhibition of the cAMP pathway
1116 decreases early long-term potentiation at CA1 hippocampal synapses. J Neurosci 20, 4446-4451.
1117 Otto, T., Eichenbaum, H., Wiener, S.I., and Wible, C.G. (1991). Learning-related patterns of CA1 spike trains
1118 parallel stimulation parameters optimal for inducing hippocampal long-term potentiation. Hippocampus
1119 1, 181-192.
1120 Papaleonidopoulos, V., Kouvaros, S., and Papatheodoropoulos, C. (2018). Effects of endogenous and
1121 exogenous D1/D5 dopamine receptor activation on LTP in ventral and dorsal CA1 hippocampal synapses.
1122 Synapse 72, e22033.
1123 Park, H., and Poo, M.M. (2013). Neurotrophin regulation of neural circuit development and function. Nat
1124 Rev Neurosci 14, 7-23.
1125 Park, P., Kang, H., Sanderson, T.M., Bortolotto, Z.A., Georgiou, J., Zhuo, M., Kaang, B.K., and Collingridge,
1126 G.L. (2018). The Role of Calcium-Permeable AMPARs in Long-Term Potentiation at Principal Neurons in
1127 the Rodent Hippocampus. Front Synaptic Neurosci 10, 42.
1128 Pattwell, S.S., Bath, K.G., Perez-Castro, R., Lee, F.S., Chao, M.V., and Ninan, I. (2012). The BDNF Val66Met
1129 Polymorphism Impairs Synaptic Transmission and Plasticity in the Infralimbic Medial Prefrontal Cortex. J
1130 Neurosci 32, 2410-2421.
1131 Pawlak, V., and Kerr, J.N. (2008). Dopamine receptor activation is required for corticostriatal spike-timing-
1132 dependent plasticity. J Neurosci 28, 2435-2446.
1133 Pike, F.G., Meredith, R.M., Olding, A.W., and Paulsen, O. (1999). Rapid report: postsynaptic bursting is
1134 essential for 'Hebbian' induction of associative long-term potentiation at excitatory synapses in rat
1135 hippocampus. J Physiol 518 (Pt 2), 571-576.
1136 Pinar, C., Fontaine, C.J., Trivino-Paredes, J., Lottenberg, C.P., Gil-Mohapel, J., and Christie, B.R. (2017).
1137 Revisiting the flip side: Long-term depression of synaptic efficacy in the hippocampus. Neurosci Biobehav
1138 Rev 80, 394-413.
1139 Plant, K., Pelkey, K.A., Bortolotto, Z.A., Morita, D., Terashima, A., McBain, C.J., Collingridge, G.L., and Isaac,
1140 J.T. (2006). Transient incorporation of native GluR2-lacking AMPA receptors during hippocampal long-
1141 term potentiation. Nat Neurosci 9, 602-604.
1142 Psotta, L., Rockahr, C., Gruss, M., Kirches, E., Braun, K., Lessmann, V., Bock, J., and Endres, T. (2015). Impact
1143 of an additional chronic BDNF reduction on learning performance in an Alzheimer mouse model. Front
1144 Behav Neurosci 9, 58.

1145 Remy, S., and Spruston, N. (2007). Dendritic spikes induce single-burst long-term potentiation. Proc Natl
1146 Acad Sci U S A 104, 17192-17197.
1147 Rosen, Z.B., Cheung, S., and Siegelbaum, S.A. (2015). Midbrain dopamine neurons bidirectionally regulate
1148 CA3-CA1 synaptic drive. Nat Neurosci 18, 1763-1771.
1149 Schildt, S., Endres, T., Lessmann, V., and Edelmann, E. (2013). Acute and chronic interference with
1150 BDNF/TrkB-signaling impair LTP selectively at mossy fiber synapses in the CA3 region of mouse
1151 hippocampus. Neuropharmacology 71, 247-254.
1152 Seol, G.H., Ziburkus, J., Huang, S., Song, L., Kim, I.T., Takamiya, K., Huganir, R.L., Lee, H.K., and Kirkwood,
1153 A. (2007). Neuromodulators control the polarity of spike-timing-dependent synaptic plasticity. Neuron 55,
1154 919-929.
1155 Shi, S., Hayashi, Y., Esteban, J.A., and Malinow, R. (2001). Subunit-specific rules governing AMPA receptor
1156 trafficking to synapses in hippocampal pyramidal neurons. Cell 105, 331-343.
1157 Shindou, T., Shindou, M., Watanabe, S., and Wickens, J. (2019). A silent eligibility trace enables dopamine-
1158 dependent synaptic plasticity for reinforcement learning in the mouse striatum. Eur J Neurosci 49, 726-
1159 736.
1160 Sivakumaran, S., Mohajerani, M.H., and Cherubini, E. (2009). At immature mossy-fiber-CA3 synapses,
1161 correlated presynaptic and postsynaptic activity persistently enhances GABA release and network
1162 excitability via BDNF and cAMP-dependent PKA. J Neurosci 29, 2637-2647.
1163 Sokoloff, P., Diaz, J., Le Foll, B., Guillin, O., Leriche, L., Bezard, E., and Gross, C. (2006). The dopamine D3
1164 receptor: a therapeutic target for the treatment of neuropsychiatric disorders. CNS Neurol Disord Drug
1165 Targets 5, 25-43.
1166 Solinas, S.M.G., Edelmann, E., Lessmann, V., and Migliore, M. (2019). A kinetic model for Brain-Derived
1167 Neurotrophic Factor mediated spike timing-dependent LTP. PLoS Comput Biol 15, e1006975.
1168 Suzuki, T., Miura, M., Nishimura, K., and Aosaki, T. (2001). Dopamine-dependent synaptic plasticity in the
1169 striatal cholinergic interneurons. J Neurosci 21, 6492-6501.
1170 Takechi, H., Eilers, J., and Konnerth, A. (1998). A new class of synaptic response involving calcium release
1171 in dendritic spines. Nature 396, 757-760.
1172 Tigaret, C.M., Olivo, V., Sadowski, J., Ashby, M.C., and Mellor, J.R. (2016). Coordinated activation of
1173 distinct Ca(2+) sources and metabotropic glutamate receptors encodes Hebbian synaptic plasticity. Nat
1174 Commun 7, 10289.
1175 Tonegawa, S., Morrissey, M.D., and Kitamura, T. (2018). The role of engram cells in the systems
1176 consolidation of memory. Nat Rev Neurosci 19, 485-498.
1177 Tritsch, N.X., and Sabatini, B.L. (2012). Dopaminergic modulation of synaptic transmission in cortex and
1178 striatum. Neuron 76, 33-50.
1179 Wang, H., Ardiles, A.O., Yang, S., Tran, T., Posada-Duque, R., Valdivia, G., Baek, M., Chuang, Y.A., Palacios,
1180 A.G., Gallagher, M.*, et al.* (2016). Metabotropic Glutamate Receptors Induce a Form of LTP Controlled by
1181 Translation and Arc Signaling in the Hippocampus. J Neurosci 36, 1723-1729.
1182 Wiera, G., Nowak, D., van Hove, I., Dziegiel, P., Moons, L., and Mozrzymas, J.W. (2017). Mechanisms of
1183 NMDA Receptor- and Voltage-Gated L-Type Calcium Channel-Dependent Hippocampal LTP Critically Rely
1184 on Proteolysis That Is Mediated by Distinct Metalloproteinases. J Neurosci 37, 1240-1256.
1185 Wittenberg, G.M., and Wang, S.S. (2006). Malleability of spike-timing-dependent plasticity at the CA3-CA1
1186 synapse. J Neurosci 26, 6610-6617.
1187 Xu, T.X., and Yao, W.D. (2010). D1 and D2 dopamine receptors in separate circuits cooperate to drive
1188 associative long-term potentiation in the prefrontal cortex. Proc Natl Acad Sci U S A 107, 16366-16371.
1189 Yang, K., and Dani, J.A. (2014). Dopamine D1 and D5 receptors modulate spike timing-dependent plasticity
1190 at medial perforant path to dentate granule cell synapses. J Neurosci 34, 15888-15897.
1191 Zhang, J.C., Lau, P.M., and Bi, G.Q. (2009). Gain in sensitivity and loss in temporal contrast of STDP by
1192 dopaminergic modulation at hippocampal synapses. Proc Natl Acad Sci U S A 106, 13028-13033.
1193